

because our patient not only had inactivation of the genes in the proximal chromosome 15 by XCI spread (including *SNRPN*) but also had a larger monosomic region of Xp21.1, although the proportion of the cells, in which the der(X) was active, was small.

Several cases with XCI spread to the translocated autosome have been reported (Orellana et al. 2001; Sharp et al. 2001; Solari et al. 2001; Stankiewicz et al. 2006). Among these cases, the majority have shown the spread of XCI in an autosome (e.g., chromosomes 10, 14, and 15) (Orellana et al. 2001; Sharp et al. 2001; Stankiewicz et al. 2006). However, a few cases have not shown such a spread (e.g., chromosomes 2 and 21) (Solari et al. 2001). Thus, it may depend on the presence of certain features that facilitate XCI spread in the vicinity of the breakpoint on an autosome (Stankiewicz et al. 2006; Wirth et al. 2001). It has been suggested that *XIST* needs some sort of genomic “way station” to aid its spread, (Gartler and Riggs 1983) and that a certain class of transposons called long interspersed (*LINE1* or *L1*) elements, (Lyon 1998) which are enriched on the X chromosome compared with autosomes, (Bailey et al. 2000; Popova et al. 2006) may be candidates for these way stations. It was recently discovered that *LINE* elements were expressed and their transcripts co-localize with the *Xist*-coated X chromosome during the X-inactivation time window in mice, *LINE1* expression was observed in an autosome around an *Xist* gene that was integrated into a mouse autosome, and the efficiency of silencing by *Xist* correlates with the local concentration of full-length and truncated *LINEs* during the establishment and maintenance of inactivation (Chow et al. 2010). If these observations are true for each gene, then the “de novo” DNA methylation in the CGI of *SNRPN* and *OCA2* may represent the high silencing efficiency of *XIST* due to the high local concentration of *LINE1*, whereas the “escape from de novo DNA methylation” in the CGI of *UBE3A* may represent the low silencing efficiency of *XIST* due to the low local concentration of *LINE1*. Contrary to the situation with *LINE1*, *Alu* repetitive elements are thought to be more enriched in genes that escape inactivation (Wang et al. 2006) and, similar to *LINE1*, *MIR* elements are found at low levels in genes that escape inactivation (Ke and Collins 2003). However, our data did not support these hypotheses because *UBE3A* did not have a higher density of *Alu* repeats or a lower density of *MIR* elements than *SNRPN* in our study. Further extensive analysis at multiple distal genes will be necessary to elucidate the “way station” hypothesis in the spread of XCI in an autosome.

Since the HUMARA assay used in this study has an error rate <5% (Kubota et al. 1999), the patient’s ratio (89:11) did not indicate a non-random (extremely skewed) XCI pattern. Thus, this result indicates the possible existence of a mosaic pattern and/or cells in which the deriva-

tive X is active. However, we did not find direct evidence for either of these possibilities, either by G-banding karyotyping (50 cells) or by replication R banding analysis (100 cells), respectively. If there are cells in which the derivative X is active and the normal X is inactive, then Xp (21.1-tel) monosomy can affect the phenotype; however, we did not observe the typical features described in females with Xp monosomy (Ogata et al. 1998), possibly because the proportion of these cells with an active derivative X and inactive normal X is low (~11%). It is also possible that some of the patient’s features (e.g., cryptorchidism and hypogonadism) may be caused by a Klinefelter-like karyotype, rather than inactivation of the PWS critical region on chromosome 15, since the patient had two X chromosomes and one Y chromosome (although one X chromosome is deleted between Xp21.1-p tel).

For the mechanism leading to the translocation, we can deduce that the initial event was a non-disjunction of the X chromosomes during maternal meiosis I, since the patient carried both maternal homologs. The translocation onto the X chromosome may be post-zygotic, given the juxtaposition of the paternal 15q on the maternal X chromosome. Furthermore, the absence of mosaicism, as determined from the cytogenetic (BrdU staining) and molecular (HUMARA assay) studies, imply the possibility that the translocation occurred very early during development, probably during the first post-zygotic divisions, as seen in a previous report (Orellana et al. 2001).

In summary, we demonstrated the extent and tendency of XCI spreading in an autosome in terms of DNA methylation using a microarray-based method. Further studies in different cases with t(X;A) translocations will contribute to a better understanding of the pathogenesis of congenital and acquired diseases, including hematological malignancies (Manola et al. 2007; Vassiliou et al. 2006) and may elucidate the properties of genes that determine whether they are subjected to or escape XCI.

Acknowledgments We thank the patient and their parents for their cooperation in this study and Professor Emeritus Tadashi Kajii for his critical reading of the manuscript. This research was supported in part by Grants-in-Aid for Scientific Research (S.S. and T.K.), Exploratory Research (T.K.) from the Ministry of Education, Culture Sports, Science, and Technology, Japan, and the Kawano foundation for medical research (T.K.), and Kawano Masanori Foundation for Promotion of Pediatrics (S.S.).

Conflict of interest None.

References

- Akahoshi K, Fukai K, Kato A, Kimiya S, Kubota T, Spritz RA (2001) Duplication of 15q11.2-q14, including the P gene, in a woman with generalized skin hyperpigmentation. *Am J Med Genet* 104:299–302

- Bailey JA, Carrel L, Chakravarti A, Eichler EE (2000) Molecular evidence for a relationship between LINE-1 elements and X chromosome inactivation: the Lyon repeat hypothesis. *Proc Natl Acad Sci USA* 97:6634–6639
- Brilliant MH, King R, Francke U, Schuffenhauer S, Meitinger T, Gardner JM, Durham-Pierre D, Nakatsu Y (1994) The mouse pink-eyed dilution gene: association with hypopigmentation in Prader-Willi and Angelman syndromes and with human OCA2. *Pigment Cell Res* 7:398–402
- Brown CJ, Ballabio A, Rupert JL, Lafreniere RG, Grompe M, Tonlorenzi R, Willard HF (1991) A gene from the region of the human X inactivation centre is expressed exclusively from the inactive X chromosome. *Nature* 349:38–44
- Chow JC, Ciaudo C, Fazzari MJ, Mise N, Servant N, Glass JL, Attreed M, Avner P, Wutz A, Barillot E, Grealley JM, Voinnet O, Heard E (2010) LINE-1 activity in facultative heterochromatin formation during X chromosome inactivation. *Cell* 141:956–969
- DuBose AJ, Johnstone KA, Smith EY, Hallett RA, Resnick JL (2010) Atp10a, a gene adjacent to the PWS/AS gene cluster, is not imprinted in mouse and is insensitive to the PWS-IC. *Neurogenetics* 11:145–151
- Gartler SM, Riggs AD (1983) Mammalian X-chromosome inactivation. *Annu Rev Genet* 17:155–190
- Giorda R, Bonaglia MC, Milani G, Baroncini A, Spada F, Beri S, Menozzi G, Rusconi M, Zuffardi O (2008) Molecular and cytogenetic analysis of the spreading of X inactivation in a girl with microcephaly, mild dysmorphic features and t(X;5)(q22.1;q31.1). *Eur J Hum Genet* 16:897–905
- Herzing LB, Romer JT, Horn JM, Ashworth A (1997) Xist has properties of the X-chromosome inactivation centre. *Nature* 386:272–275
- Ke X, Collins A (2003) CpG islands in human X-inactivation. *Ann Hum Genet* 67:242–249
- Kubota T, Nonoyama S, Tonoki H, Masuno M, Imaizumi K, Kojima M, Wakui K, Shimadzu M, Fukushima Y (1999) A new assay for the analysis of X-chromosome inactivation based on methylation-specific PCR. *Hum Genet* 104:49–55
- Kubota T, Wakui K, Nakamura T, Ohashi H, Watanabe Y, Yoshino M, Kida T, Okamoto N, Matsumura M, Muroya K, Ogata T, Goto Y, Fukushima Y (2002) The proportion of cells with functional X disomy is associated with the severity of mental retardation in mosaic ring X Turner syndrome females. *Cytogenet Genome Res* 99:276–284
- Lee JT, Jaenisch R (1997) Long-range cis effects of ectopic X-inactivation centres on a mouse autosome. *Nature* 386:275–279
- Lee JT, Strauss WM, Dausman JA, Jaenisch R (1996) A 450 kb transgene displays properties of the mammalian X-inactivation center. *Cell* 86:83–94
- Lyon MF (1961) Gene action in the X-chromosome of the mouse (*Mus musculus* L.). *Nature* 190:372–373
- Lyon MF (1962) Sex chromatin and gene action in the mammalian X-chromosome. *Am J Hum Genet* 14:135–148
- Lyon MF (1998) X-chromosome inactivation: a repeat hypothesis. *Cytogenet Cell Genet* 80:133–137
- Manola KN, Stavropoulou C, Georgakakos VN, Zoi K, Fisis M, Evmorfiadis I, Zoi C, Pantelias GE, Stefanoudaki K, Sambani C (2007) Switch in X-inactivation in a JAK2 V617F-negative case of polycythemia vera with two acquired X-autosome translocations. *Leuk Res* 31:1009–1014
- Ogata T, Wakui K, Muroya K, Ohashi H, Matsuo N, Brown DM, Ishii T, Fukushima Y (1998) Microphthalmia with linear skin defects syndrome in a mosaic female infant with monosomy for the Xp22 region: molecular analysis of the Xp22 breakpoint and the X-inactivation pattern. *Hum Genet* 103:51–56
- Orellana C, Martinez F, Badia L, Millan JM, Montero MR, Andres J, Prieto F (2001) Trisomy rescue by postzygotic unbalanced (X;14) translocation in a girl with dysmorphic features. *Clin Genet* 60:206–211
- Popova BC, Tada T, Takagi N, Brockdorff N, Nesterova TB (2006) Attenuated spread of X-inactivation in an X;autosome translocation. *Proc Natl Acad Sci USA* 103:7706–7711
- Schmidt M, Du Sart D (1992) Functional disomies of the X chromosome influence the cell selection and hence the X inactivation pattern in females with balanced X-autosome translocations: a review of 122 cases. *Am J Med Genet* 42:161–169
- Sharp A, Robinson DO, Jacobs P (2001) Absence of correlation between late-replication and spreading of X inactivation in an X;autosome translocation. *Hum Genet* 109:295–302
- Sharp AJ, Spotswood HT, Robinson DO, Turner BM, Jacobs PA (2002) Molecular and cytogenetic analysis of the spreading of X inactivation in X;autosome translocations. *Hum Mol Genet* 11:3145–3156
- Sharp AJ, Migliavacca E, Dupre Y, Stathaki E, Sailani MR, Baumer A, Schinzel A, Mackay DJ, Robinson DO, Cobellis G, Cobellis L, Brunner HG, Steiner B, Antonarakis SE (2010) Methylation profiling in individuals with uniparental disomy identifies novel differentially methylated regions on chromosome 15. *Genome Res* 20:1271–1278
- Solari AJ, Rahn IM, Ferreyra ME, Carballo MA (2001) The behavior of sex chromosomes in two human X-autosome translocations: failure of extensive X-inactivation spreading. *Biocell* 25:155–166
- Stankiewicz P, Kuechler A, Eller CD, Sahoo T, Baldermann C, Lieser U, Hesse M, Glaser C, Hagemann M, Yatsenko SA, Liehr T, Horsthemke B, Claussen U, Marahrens Y, Lupski JR, Hansmann I (2006) Minimal phenotype in a girl with trisomy 15q due to t(X;15)(q22.3;q11.2) translocation. *Am J Med Genet A* 140:442–452
- Takagi N, Abe K (1990) Detrimental effects of two active X chromosomes on early mouse development. *Development* 109:189–201
- Uehara S, Hanew K, Harada N, Yamamori S, Nata M, Niikawa N, Okamura K (2001) Isochromosome consisting of terminal short arm and proximal long arm X in a girl with short stature. *Am J Med Genet* 99:196–199
- Vassiliou GS, Campbell PJ, Li J, Roberts I, Swanton S, Huntly BJ, Fourouclas N, Baxter EJ, Munro LR, Culligan DA, Scott LM, Green AR (2006) An acquired translocation in JAK2 Val617Phe-negative essential thrombocythemia associated with autosomal spread of X-inactivation. *Haematologica* 91:1100–1104
- Wang Z, Willard HF, Mukherjee S, Furey TS (2006) Evidence of influence of genomic DNA sequence on human X chromosome inactivation. *PLoS Comput Biol* 2:e113
- White WM, Willard HF, Van Dyke DL, Wolff DJ (1998) The spreading of X inactivation into autosomal material of an x;autosome translocation: evidence for a difference between autosomal and X-chromosomal DNA. *Am J Hum Genet* 63:20–28
- Wirth J, Back E, Huttenhofer A, Nothwang HG, Lich C, Gross S, Menzel C, Schinzel A, Kioschis P, Tommerup N, Ropers HH, Horsthemke B, Buiting K (2001) A translocation breakpoint cluster disrupts the newly defined 3' end of the SNURF-SNRPN transcription unit on chromosome 15. *Hum Mol Genet* 10:201–210
- Xue F, Tian XC, Du F, Kubota C, Taneja M, Dinnyes A, Dai Y, Levine H, Pereira LV, Yang X (2002) Aberrant patterns of X chromosome inactivation in bovine clones. *Nat Genet* 31:216–220
- Yang X, Smith SL, Tian XC, Lewin HA, Renard JP, Wakayama T (2007) Nuclear reprogramming of cloned embryos and its implications for therapeutic cloning. *Nat Genet* 39:295–302

Submicroscopic Deletion in 7q31 Encompassing *CADPS2* and *TSPAN12* in a Child With Autism Spectrum Disorder and PHPV

Nobuhiko Okamoto,^{1*} Yoshikazu Hatsukawa,² Keiko Shimojima,³ and Toshiyuki Yamamoto³

¹Department of Medical Genetics, Osaka Medical Center and Research Institute for Maternal and Child Health, Osaka, Japan

²Department of Ophthalmology, Osaka Medical Center and Research Institute for Maternal and Child Health, Osaka, Japan

³Institute for Integrated Medical Sciences, Tokyo Women's Medical University, Tokyo, Japan

Received 23 August 2010; Accepted 9 March 2011

We performed array comparative genomic hybridization utilizing a whole genome oligonucleotide microarray in a patient with the autism spectrum disorders (ASDs) and persistent hyperplastic primary vitreous (PHPV). Submicroscopic deletions in 7q31 encompassing *CADPS2* (Ca²⁺-dependent activator protein for secretion 2) and *TSPAN12* (one of the members of the tetraspanin superfamily) were confirmed. The *CADPS2* plays important roles in the release of neurotrophin-3 and brain-derived neurotrophic factor. Mutations in *TSPAN12* are a relatively frequent cause of familial exudative vitreoretinopathy. We speculate that haploinsufficiency of *CADPS2* and *TSPAN12* contributes to ASDs and PHPV, respectively.

© 2011 Wiley-Liss, Inc.

Key words: *CADPS2*; *TSPAN12*; autism; PHPV; CGH

INTRODUCTION

Autism spectrum disorders (ASDs OMIM %209850) are complex neurodevelopmental conditions characterized by social communication disabilities, no or delayed language development, and stereotyped and repetitive behaviors. A number of studies have confirmed that genetic factors play an important role in ASDs.

About 10% of ASDs are associated with a Mendelian syndrome (e.g., fragile X syndrome, tuberous sclerosis and Timothy syndrome). Cytogenetic approaches revealed a high frequency of large chromosomal abnormalities (3–7% of patients), including the most frequently observed maternal 15q11-13 duplication (1–3% of patients). Association studies and mutation analysis of candidate genes have implicated the synaptic genes *NLGN3* (Neurologin3 OMIM*300336), *NLGN4* (OMIM*300427) [Jamain et al., 2003], *SHANK3* (OMIM*606230) [Durand et al., 2007; Moessner et al., 2007], *NRXN1* (Neurexin1 MIM + 600565) [Kim et al., 2008], *SHANK2* (OMIM*603290) [Berkel et al., 2010], and *CNTNAP2* (MIM*604569) [Alarcón et al., 2008; Arking et al., 2008] in ASDs. There is increasing evidence that the *SHANK3-NLGN4-NRXN1* postsynaptic density genes play important roles in the pathogenesis of ASDs.

How to Cite this Article:

Okamoto N, Hatsukawa Y, Shimojima K, Yamamoto T. 2011. Submicroscopic deletion in 7q31 encompassing *CADPS2* and *TSPAN12* in a child with autism spectrum disorder and PHPV.

Am J Med Genet Part A 155:1568–1573.

Recently, an association between de novo copy number variation (CNV) and ASDs was revealed. Sebat et al. [2007] performed comparative genomic hybridization (CGH) on the genomic DNA from ASD patients and unaffected subjects to detect de novo CNV. As a result, they identified CNV in 12 out of 118 (10%) patients with sporadic ASD and confirmed de novo CNV were significantly associated with ASDs. Marshall et al. [2008] performed a genome-wide search for structural abnormalities in 427 unrelated ASD patients using SNP microarray analysis and karyotyping. De novo CNV were found in approximately 7% and approximately 2% of idiopathic families with one ASD child, or two or more ASD siblings, respectively. These authors discovered a CNV at 16p11.2 with an approximate frequency of 1%. Glessner et al. [2009] reported the results from a whole-genome CNV study of many European ASD patients and controls and found several new susceptibility genes encoding neuronal cell-adhesion molecules, including *NLGN1* and *ASTN2*, and genes involved in the ubiquitin pathways, including *UBE3A*, *PARK2*, *RFWD2*, and *FBXO40*. The investigators suggested that two gene networks, neuronal cell-

Grant sponsor: Ministry of Health, Labour and Welfare of Japan.

*Correspondence to:

Nobuhiko Okamoto, Department of Medical Genetics, Osaka Medical Center and Research Institute for Maternal and Child Health, 840 Murodocho, Izumi, Osaka 594-1101, Japan. E-mail: okamoto@osaka.email.ne.jp

Published online 27 May 2011 in Wiley Online Library

(wileyonlinelibrary.com).

DOI 10.1002/ajmg.a.34028

adhesion and ubiquitin degradation, that are expressed within the central nervous system contribute to the genetic susceptibility of ASDs.

The International Molecular Genetic Study of Autism Consortium [1998] previously identified linkage loci on chromosomes 7 and 2, which were termed AUTS1 and AUTS5, respectively. Further genetic studies have provided evidence for AUTS1 being located on chromosome 7q [The International Molecular Genetic Study of Autism Consortium 2001]. Screening for mutations in six genes mapping to 7q, *CUTLI*, *SRPK2*, *SYPL*, *LAMBI*, *NRCAM*, and *PTPRZ1* in 48 unrelated individuals with autism led to the identification of several new coding variants in the *CUTLI*, *LAMBI*, and *PTPRZ1* genes [Bonora et al., 2005].

The human Ca^{2+} -dependent activator protein for secretion 2 (*CADPS2*: OMIM*609978) is also located on chromosome 7q31, which is within the AUTS1 locus [Cisternas et al., 2003]. It is a member of the CAPS/CADPS protein family that regulates the secretion of dense-core vesicles, which are abundant in the parallel fiber terminals of granule cells in the cerebellum and play important roles in the release of neurotrophin-3 (NT-3) and brain-derived neurotrophic factor (BDNF) [Sadakata et al., 2007a,b,c]. BDNF is indispensable for brain development and function, including the formation of synapses. Cisternas et al. [2003] studied *CADPS2* mutations in 90 unrelated autistic individuals, but identified no disease-specific variants. However, Sadakata et al. [2007a] reported that an aberrant, alternatively spliced *CADPS2* mRNA that lacks exon 3 (*CADPS2* Delta exon3) is detected in some patients with ASD.

Persistent hyperplastic primary vitreous (PHPV) is an ocular malformation caused by the presence of a retrolental fibrovascular membrane and the persistence of the posterior portion of the tunica vasculosa lentis and the hyaloid artery. It is often accompanied by microphthalmos, cataracts, and glaucoma. *NDP* (OMIM *300658, X-linked) and *FZD4* (OMIM *604579, dominant) were found to be mutated in unilateral and bilateral PHPV [Shastry, 2009]. These genes also cause Norrie disease and familial exudative vitreoretinopathy (FEVR), which share some clinical features with PHPV. FEVR is a genetically heterogeneous retinal disorder characterized by abnormal vascularization of the peripheral retina, which is often accompanied by retinal detachment. Mutations in the genes encoding *LRP5* (OMIM *603506, dominant and recessive) also cause FEVR. Junge et al. [2009] showed that *Tetraspanin12* (*Tspan12*) is expressed in the retinal vasculature, and loss of *Tspan12* phenocopies defects are seen in *Fzd4*, *Lrp5*, and *Norrin* mutant mice. *TSPAN12* is one of the members of the tetraspanin superfamily, characterized by the presence of four transmembrane domains. It constitutes large membrane complexes with other molecules. Nikopoulos et al. [2010] applied next-generation sequencing and found a mutation in *TSPAN12* (MIM*613168). Poulter et al. [2010] described seven mutations that were identified in a cohort of 70 FEVR patients without mutations in three known genes. Mutations in *TSPAN12*, which is at 7q31, are a relatively frequent cause of FEVR.

We performed array comparative genomic hybridization (array-CGH) utilizing a 44K whole genome oligonucleotide microarray in a patient with the ASDs and PHPV. Submicroscopic deletions in 7q31 encompassing *CADPS2* and *TSPAN12* were confirmed. We

speculate that haploinsufficiency of *CADPS2* and *TSPAN12* contributes to ASD and PHPV, respectively.

CLINICAL REPORT

The patient, a 3-year-old boy, was born to nonconsanguineous healthy Japanese parents. His family history was unremarkable. He was born at 40 weeks' of gestation, his birth weight was 3,100 g, and his birth length was 50.0 cm. After birth, congenital nystagmus was noted, and he did not pursue objects. An ophthalmological examination revealed bilateral PHPV. Cataract, glaucoma, and FEVR were not present. His gross motor development was normal, and his verbal development was delayed.

At 3 years of age, he came to our hospital for evaluation because of developmental delay. On examination dysmorphic features included a round face, low-set ears, broad eyebrows, apparent hypertelorism, blepharophimosis, hypoplastic alae nasi, a long philtrum, and a small mouth. His visual acuity was low, but he could perform daily activities with some support. In addition, impairment of social interaction, poor social skills, and strict adherence to routine behaviors were noted. He showed stereotypic movements and hyperactivity in his day care room. He was diagnosed as having an ASD according to the DSM-VI criteria. His DQ was 76 according to standard Japanese method. At 3 years and 8 months of age, his height, weight, and head circumference were 88.6 cm (-2.4 SD), 11.7 kg (-1.8 SD), and 46.8 cm (-2.4 S.D.), respectively.

The results of routine laboratory tests were unremarkable. G-banded karyotype analysis revealed the following karyotype: 46,XY,inv(4)(p14;q21). Electroencephalography (EEG) showed occipital epileptic discharges. He was free from epileptic seizures.

Ultrasound evaluation revealed echogenic bands in the posterior segments of both globes. Magnetic resonance brain imaging also showed bilateral fibrous intraocular tissue (Fig. 1). However, no specific findings were found in the CNS including the cerebellum.

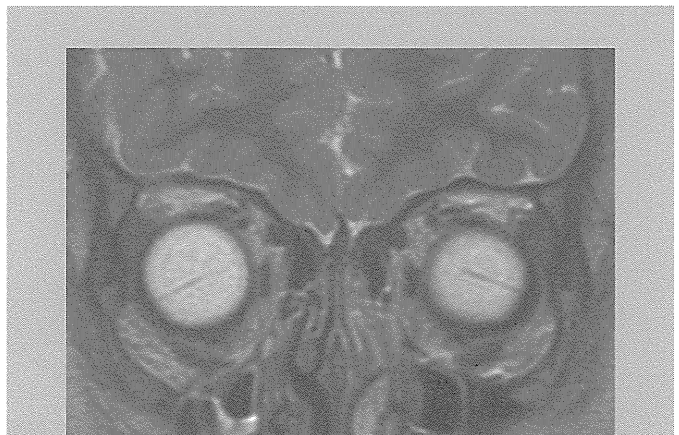


FIG. 1. MR coronal image, T2-weighted. Magnetic resonance imaging also showed fibrous intraocular tissue in the eye. [Color figure can be seen in the online version of this article, available at [http://onlinelibrary.wiley.com/journal/10.1002/\(ISSN\)1552-4833](http://onlinelibrary.wiley.com/journal/10.1002/(ISSN)1552-4833)]

MATERIALS AND METHODS

After obtaining informed consent based on a permission approved by the institution's ethical committee, peripheral blood samples were obtained from the patient and his parents. Genomic DNA was extracted using the QIAquick DNA extraction kit (QIAGEN, Valencia, CA).

Array-CGH analysis was performed using the Human Genome CGH Microarray 44K (Agilent Technologies, Santa Clara, CA), as described previously [Shimajima et al., 2009].

Metaphase nuclei were prepared from peripheral blood lymphocytes using standard methods and were used for FISH analysis with human BAC clones selected from the UCSC genome browser (<http://www.genome.ucsc.edu>), as described elsewhere [Shimajima et al., 2009]. Physical positions refer to the March 2006 human reference sequence (NCBI Build 36.1).

RESULTS

Using array-CGH analysis, genomic copy number loss was identified in the 7q31.31 region (Fig. 2). The deletion was 5.4 Mb in size and included *CADPS2* and *TSPAN12*, but not *FOXP2*. There were no copy number changes in chromosome 4. FISH analyses confirmed the above deletion (Fig. 3). There were no deletions in either parent indicating de novo occurrence.

DISCUSSION

We described a patient with an ASD and PHPV who demonstrated submicroscopic deletion in chromosome 7q31.31. The deletion resides in the *AUTS1* locus on chromosome 7q. The deleted region contained about 20 genes including *CADPS2* and *TSPAN12*. Little data are available about the association of other genes with developmental and ophthalmological disorders. We posit that haploinsufficiency of *CADPS2* and *TSPAN12* contributes to ASDs and PHPV, respectively.

Our patient fulfilled the DSM-VI criteria for an ASD. Poor eye contact, impairment of social interaction, poor social skills with strict adherence to routine, stereotypic movements, and hyperactivity were noted. However, his intellectual disability was mild. Ataxic movement was not observed.

There have been several reports of small deletions on chromosome 7q. Lennon et al. [2007] reported a young male with moderate intellectual disability, dysmorphic features, and language delay who had a deletion in the 7q31.1-7q31.31 region, which included the *FOXP2* gene. The patient demonstrated language impairment, including developmental verbal dyspraxia, but did not meet the criteria for autism. Cukier et al. [2009] reported a chromosomal inversion spanning the region from approximately 7q22.1 to 7q31 in autistic siblings. They suggested that an autism susceptibility gene is located in the chromosome 7q22-31 region. Dauwerse et al.

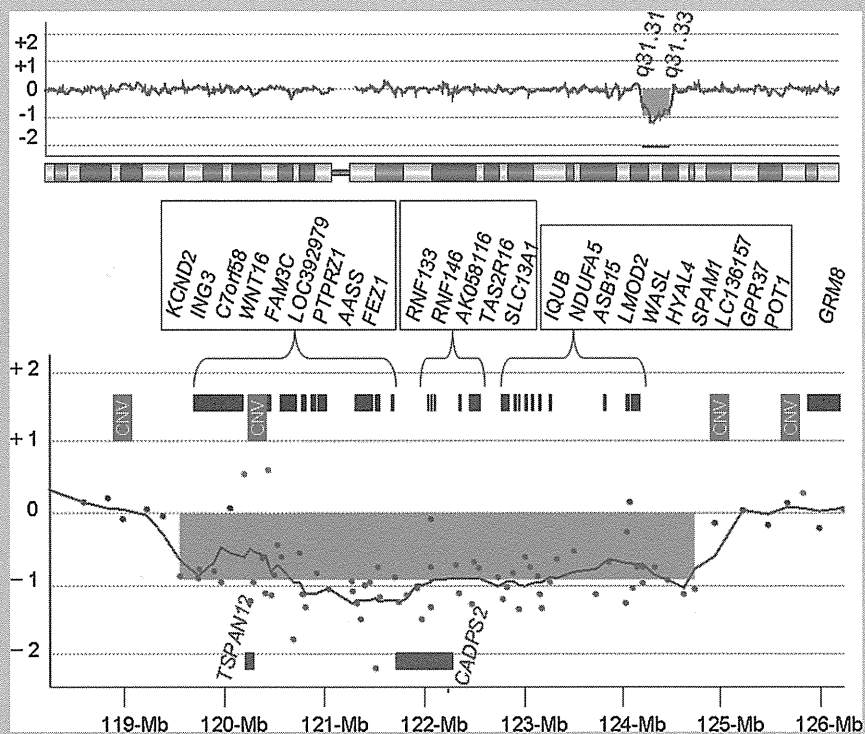


FIG. 2. Array-CGH of the patient. Loss of the genomic copy numbers was identified in the region of 7q31.31. The deletion size was 5.4 Mb and included *CADPS2* and *TSPAN12*.

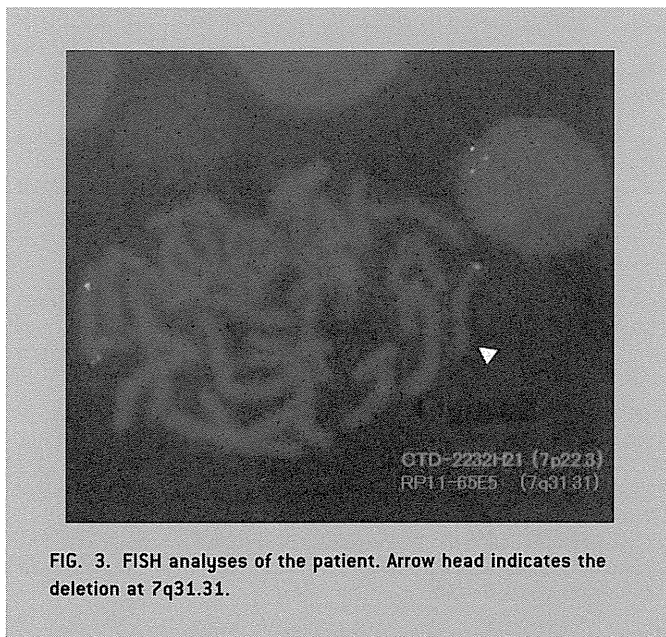


FIG. 3. FISH analyses of the patient. Arrow head indicates the deletion at 7q31.31.

[2010] characterized a de novo complex rearrangement of the long arm of chromosome 7 in a female patient with moderate mental retardation, anxiety disorder, and autistic features and suggested that disruption of the *C7orf58* gene contributed to the anxiety disorder, and autistic features of their patient. The *C7orf58* gene was also deleted in our patient. However, there have been no basic studies on the association of the *C7orf58* gene and brain function. Further studies are necessary on the role of the *C7orf58* gene.

Sadakata et al. [2007b] studied the behavior of *Cadps2*^{-/-} mice. They showed impaired social interaction, hyperactivity, decreased exploratory behavior, and/or increased anxiety in a novel environment and deficits in intrinsic sleep-wake regulation and circadian rhythmicity. In addition, maternal neglect of newborns was a striking feature. They identified that *Cadps2*^{-/-} mice show deficient release of NT-3 and BDNF. Cerebellar development was impaired in the mice. Sadakata et al. [2007a] found an aberrant alternatively spliced *CADPS2* mRNA that lacks exon 3 in some autistic patients. Exon 3 was shown to encode the dynactin 1-binding domain and affect axonal *CADPS2* protein distribution. Exon 3-skipped *CADPS2* protein possesses almost normal BDNF releasing activity but is not properly transported into the axons of neocortical or cerebellar neurons. However, Eran et al. [2009] observed no difference in prevalence of exon 3 skipping between ASDs and control samples. They concluded that exon 3 skipping represents a normal, minor isoform of *CADPS2* in the cerebellum and is likely not a mechanism underlying autism susceptibility or pathogenesis. Our result may reinforce the evidence that *CADPS2* is associated with ASDs.

Cisternas et al. [2003] studied *CADPS2* gene mutations in 90 unrelated autistic individuals. However, they identified no disease-specific variants. Their results indicate that *CADPS2* mutations are not a major cause of ASDs. However, although small deletions of *CADPS2* as found in the present patient, might be rare, they support the idea that *CADPS2* abnormalities are associated with autism susceptibility.

Nikopoulos et al. [2010] reported two missense mutations in five of 11 FEVR families, indicating that mutations in *TSPAN12* are a relatively frequent cause of FEVR. Both residues are completely conserved throughout vertebrate evolution. These authors suggested that both haploinsufficiency and a dominant-negative effect of the mutant *TSPAN12* on the wild-type protein should be considered as underlying disease mechanisms. Poulter et al. [2010] described mutations in the *TSPAN12* gene in FEVR patients and suggested that haploinsufficiency of *TSPAN12* causes FEVR because at least four of the seven mutations are predicted to lead to transcripts with premature-termination codons that are likely to be targeted by nonsense-mediated decay.

Recently, the Norrin/Frizzled4 signaling pathway that acts on the surface of developing endothelial cells and controls retinal vascular development is highlighted [Ye et al., 2010]. This pathway is composed of Norrin, its transmembrane receptor, Frizzled4, coreceptor, Lrp5, and an auxiliary membrane protein, Tspan12. The resulting signal controls a transcriptional program that regulates endothelial growth and maturation. PHPV and FEVR are associated with their pathogenesis. Our findings indicate that haploinsufficiency of *TSPAN12* is a plausible causative mechanism for PHPV. It will be interesting to study *TSPAN12* abnormalities in PHPV without *NDP* and *FZD4* mutations.

Singh et al. [2006] reported a voltage-gated potassium channel gene mutation in a temporal lobe epilepsy patient, namely a Kv4.2 truncation mutation lacking the last 44 amino acids in the carboxyl terminal. Kv4.2 channel is encoded by the *KCND2* gene. We suggest that the epileptic discharges on EEG reflect neuronal excitability caused by haploinsufficiency of *KCND2*.

Shen et al. [2010] suggested that using chromosomal microarray analysis to test for submicroscopic genomic deletions and duplications should be considered as part of the initial diagnostic evaluation of patients with ASDs. Miller et al. [2010] suggested that the use of chromosomal microarray is recommended as the first-tier cytogenetic diagnostic test for patients with unexplained developmental delay/intellectual disability, ASDs, or multiple congenital anomalies. In patients with ASDs and other anomalies, chromosomal microarray may be the useful method to clarify the underlying defect.

ACKNOWLEDGMENTS

We thank the patient's family for their cooperation. This study was supported by Health and Labour Research Grants from the Ministry of Health, Labour and Welfare of Japan.

REFERENCES

- Alarcón M, Abrahams BS, Stone JL, Duvall JA, Perederiy JV, Bomar JM, Sebat J, Wigler M, Martin CL, Ledbetter DH, Nelson SF, Cantor RM, Geschwind DH. 2008. Linkage, association, and gene-expression analyses identify *CNTNAP2* as an autism-susceptibility gene. *Am J Hum Genet* 82:150–159.
- Arking DE, Cutler DJ, Brune CW, Teslovich TM, West K, Ikeda M, Rea A, Guy M, Lin S, Cook EH, Chakravarti A. 2008. A common genetic variant in the neurexin superfamily member *CNTNAP2* increases familial risk of autism. *Am J Hum Genet* 82:160–164.

- Berkel S, Marshall CR, Weiss B, Howe J, Roeth R, Moog U, Endris V, Roberts W, Szatmari P, Pinto D, Bonin M, Riess A, Engels H, Sprengel R, Scherer SW, Rappold GA. 2010. Mutations in the SHANK2 synaptic scaffolding gene in autism spectrum disorder and mental retardation. *Nat Genet* 42:489–491.
- Bonora E, Lamb JA, Barnby G, Sykes N, Moberly T, Beyer KS, Klauck SM, Poustka F, Bacchelli E, Blasi F, Maestrini E, Battaglia A, Haracopos D, Pedersen L, Isager T, Eriksen G, Viskum B, Sorensen EU, Brondum-Nielsen K, Cotterill R, Engeland H, Jonge M, Kemner C, Stegheuis K, Scherpenisse M, Rutter M, Bolton PF, Parr JR, Poustka A, Bailey AJ, Monaco AP, International Molecular Genetic Study of Autism Consortium. 2005. Mutation screening and association analysis of six candidate genes for autism on chromosome 7q. *Eur J Hum Genet* 13:198–207.
- Cisternas FA, Vincent JB, Scherer SW, Ray PN. 2003. Cloning and characterization of human CADPS and CADPS2, new members of the Ca²⁺-dependent activator for secretion protein family. *Genomics* 81:279–291.
- Cukier HN, Skaar DA, Rayner-Evans MY, Konidari I, Whitehead PL, Jaworski JM, Cuccaro ML, Pericak-Vance MA, Gilbert JR. 2009. Identification of chromosome 7 inversion breakpoints in an autistic family narrows candidate region for autism susceptibility. *Autism Res* 2:258–266.
- Dauwse JG, Ruivenkamp CA, Hansson K, Marijnissen GM, Peters DJ, Breuning MH, Hilhorst-Hofstee Y. 2010. A complex chromosome 7q rearrangement identified in a patient with mental retardation, anxiety disorder, and autistic features. *Am J Med Genet Part A* 152A:427–433.
- Durand CM, Betancur C, Boeckers TM, Bockmann J, Chaste P, Fauchereau F, Nygren G, Rastam M, Gillberg IC, Anckarsäter H, Sponheim E, Goubran-Botros H, Delorme R, Chabane N, Mouren-Simeoni MC, de Mas P, Bieth E, Rogé B, Héron D, Burglen L, Gillberg C, Leboyer M, Bourgeron T. 2007. Mutations in the gene encoding the synaptic scaffolding protein SHANK3 are associated with autism spectrum disorders. *Nat Genet* 39:25–27.
- Eran A, Graham KR, Vatalaro K, McCarthy J, Collins C, Peters H, Brewster SJ, Hanson E, Hundley R, Rappaport L, Holm IA, Kohane IS, Kunkel LM. 2009. Comment on “Autistic-like phenotypes in *Cadps2*-knockout mice and aberrant CADPS2 splicing in autistic patients”. *J Clin Invest* 119:679–680.
- Glessner JT, Wang K, Cai G, Korvatska O, Kim CE, Wood S, Zhang H, Estes A, Brune CW, Bradfield JP, Imielinski M, Frackelton EC, Reichert J, Crawford EL, Munson J, Sleiman PM, Chiavacci R, Annaiah K, Thomas K, Hou C, Glaberson W, Flory J, Otieno F, Garriss M, Soorya L, Klei L, Piven J, Meyer KJ, Anagnostou E, Sakurai T, Game RM, Rudd DS, Zurawiecki D, McDougle CJ, Davis LK, Miller J, Posey DJ, Michaels S, Kolevzon A, Silverman JM, Bernier R, Levy SE, Schultz RT, Dawson G, Owley T, McMahon WM, Wassink TH, Sweeney JA, Nurnberger JL, Coon H, Sutcliffe JS, Minshew NJ, Grant SF, Bucan M, Cook EH, Buxbaum JD, Devlin B, Schellenberg GD, Hakonarson H. 2009. Autism genome-wide copy number variation reveals ubiquitin and neuronal genes. *Nature* 459:569–573.
- International Molecular Genetic Study of Autism Consortium. 1998. A full genome screen for autism with evidence for linkage to a region on chromosome 7q. *Hum Mol Genet* 7:571–578.
- International Molecular Genetic Study of Autism Consortium (IMGSAC). 2001. Further characterization of the autism susceptibility locus AUTS1 on chromosome 7q. *Hum Mol Genet* 10:973–982.
- Jamain S, Quach H, Betancur C, Rastam M, Colineaux C, Gillberg IC, Soderstrom H, Giros B, Leboyer M, Gillberg C, Bourgeron T. Paris Autism Research International Sibpair Study. 2003. Mutations of the X-linked genes encoding neuroligins NLGN3 and NLGN4 are associated with autism. *Nat Genet* 34:27–29.
- Junge HJ, Yang S, Burton JB, Paes K, Shu X, French DM, Costa M, Rice DS, Ye W. 2009. TSPAN12 regulates retinal vascular development by promoting Norrin- but not Wnt-induced FZD4/beta-catenin signaling. *Cell* 139:299–311.
- Kim HG, Kishikawa S, Higgins AW, Seong IS, Donovan DJ, Shen Y, Lally E, Weiss LA, Najm J, Kutsche K, Descartes M, Holt L, Braddock S, Troxell R, Kaplan L, Volkmar F, Klin A, Tsatsanis K, Harris DJ, Noens I, Pauls DL, Daly MJ, MacDonald ME, Morton CC, Quade BJ, Gusella JF. 2008. Disruption of neurexin 1 associated with autism spectrum disorder. *Am J Hum Genet* 82:199–207.
- Lennon PA, Cooper ML, Peiffer DA, Gunderson KL, Patel A, Peters S, Cheung SW, Bacino CA. 2007. Deletion of 7q31.1 supports involvement of FOXP2 in language impairment: Clinical report and review. *Am J Med Genet A* 143A:791–798.
- Marshall CR, Noor A, Vincent JB, Lionel AC, Feuk L, Skaug J, Shago M, Moessner R, Pinto D, Ren Y, Thiruvahindrapuram B, Fiebig A, Schreiber S, Friedman J, Ketelaars CE, Vos YJ, Ficicoglu C, Kirkpatrick S, Nicolson R, Sloman L, Summers A, Gibbons CA, Teebi A, Chitayat D, Weksberg R, Thompson A, Vardy C, Crosbie V, Luscombe S, Baatjes R, Zwaigenbaum L, Roberts W, Fernandez B, Szatmari P, Scherer SW. 2008. Structural variation of chromosomes in autism spectrum disorder. *Am J Hum Genet* 82:477–488.
- Miller DT, Adam MP, Aradhya S, Biesecker LG, Brothman AR, Carter NP, Church DM, Crolla JA, Eichler EE, Epstein CJ, Faucett WA, Feuk L, Friedman JM, Hamosh A, Jackson L, Kaminsky EB, Kok K, Krantz ID, Kuhn RM, Lee C, Ostell JM, Rosenberg C, Scherer SW, Spinner NB, Stavropoulos DJ, Tepperberg JH, Thorland EC, Vermeech JR, Waggoner DJ, Watson MS, Martin CL, Ledbetter DH. 2010. Consensus statement: Chromosomal microarray is a first-tier clinical diagnostic test for individuals with developmental disabilities or congenital anomalies. *Am J Hum Genet* 86:749–764.
- Moessner R, Marshall CR, Sutcliffe JS, Skaug J, Pinto D, Vincent J, Zwaigenbaum L, Fernandez B, Roberts W, Szatmari P, Scherer SW. 2007. Contribution of SHANK3 mutations to autism spectrum disorder. *Am J Hum Genet* 81:1289–1297.
- Nikopoulos K, Gilissen C, Hoischen A, van Nouhuys CE, Boonstra FN, Blokland EA, Arts P, Wieskamp N, Strom TM, Ayuso C, Tilanus MA, Bouwhuis S, Mukhopadhyay A, Scheffer H, Hoefsloot LH, Veltman JA, Cremers FP, Collin RW. 2010. Next-generation sequencing of a 40 Mb linkage interval reveals TSPAN12 mutations in patients with familial exudative vitreoretinopathy. *Am J Hum Genet* 86:240–247.
- Poulter JA, Ali M, Gilmour DF, Rice A, Kondo H, Hayashi K, Mackey DA, Kearns LS, Ruddell JB, Craig JE, Pierce EA, Downey LM, Mohamed MD, Markham AF, Inglehearn CF, Toomes C. 2010. Mutations in TSPAN12 cause autosomal-dominant familial exudative vitreoretinopathy. *Am J Hum Genet* 86:248–253.
- Sadakata T, Washida M, Iwayama Y, Shoji S, Sato Y, Ohkura T, Katoh-Semba R, Nakajima M, Sekine Y, Tanaka M, Nakamura K, Iwata Y, Tsuchiya KJ, Mori N, Detera-Wadleigh SD, Ichikawa H, Itohara S, Yoshikawa T, Furuichi T. 2007a. Autistic-like phenotypes in *Cadps2*-knockout mice and aberrant CADPS2 splicing in autistic patients. *J Clin Invest* 117:931–943.
- Sadakata T, Kakegawa W, Mizoguchi A, Washida M, Katoh-Semba R, Shutoh F, Okamoto T, Nakashima H, Kimura K, Tanaka M, Sekine Y, Itohara S, Yuzaki M, Nagao S, Furuichi T. 2007b. Impaired cerebellar development and function in mice lacking CAPS2, a protein involved in neurotrophin release. *J Neurosci* 27:2472–2482.
- Sadakata T, Washida M, Furuichi T. 2007c. Alternative splicing variations in mouse CAP S2: Differential expression and functional properties of splicing variants. *BMC Neurosci* 8:25.
- Sebat J, Lakshmi B, Malhotra D, Troge J, Lese-Martin C, Walsh T, Yamrom B, Yoon S, Krasnitz A, Kendall J, Leotta A, Pai D, Zhang R, Lee YH, Hicks

- J, Spence SJ, Lee AT, Puura K, Lehtimäki T, Ledbetter D, Gregersen PK, Bregman J, Sutcliffe JS, Jobanputra V, Chung W, Warburton D, King MC, Skuse D, Geschwind DH, Gilliam TC, Ye K, Wigler M. 2007. Strong association of de novo copy number mutations with autism. *Science* 316:445–449.
- Shastri BS. 2009. Persistent hyperplastic primary vitreous: Congenital malformation of the eye. *Clin Experiment Ophthalmol* 37:884–890.
- Shen Y, Dies KA, Holm IA, Bridgemohan C, Sobeih MM, Caronna EB, Miller KJ, Frazier JA, Silverstein I, Picker J, Weissman L, Raffalli P, Jeste S, Demmer LA, Peters HK, Brewster SJ, Kowalczyk SJ, Rosen-Sheidley B, McGowan C, Duda AW III, Lincoln SA, Lowe KR, Schonwald A, Robbins M, Hisama F, Wolff R, Becker R, Nasir R, Urion DK, Milunsky JM, Rappaport L, Gusella JF, Walsh CA, Wu BL, Miller DT. Autism Consortium Clinical Genetics/DNA Diagnostics Collaboration. 2010. Clinical genetic testing for patients with autism spectrum disorders. *Pediatrics* 125:e727–e735.
- Shimajima K, Páez MT, Kurosawa K, Yamamoto T. 2009. Proximal interstitial 1p36 deletion syndrome: The most proximal 3.5-Mb micro-deletion identified on a dysmorphic and mentally retarded patient with inv(3)(p14.1q26.2). *Brain Development* 31:629–633.
- Singh B, Ogiwara I, Kaneda M, Tokonami N, Mazaki E, Baba K, Matsuda K, Inoue Y, Yamakawa K. 2006. A Kv4.2 truncation mutation in a patient with temporal lobe epilepsy. *Neurobiol Dis* 24:245–253.
- Ye X, Wang Y, Nathans J. 2010. The Norrin/Frizzled4 signaling pathway in retinal vascular development and disease. *Trends Mol Med* 16:417–425.

Submicroscopic Deletion of 12q13 Including *HOXC* Gene Cluster With Skeletal Anomalies and Global Developmental Delay

Nobuhiko Okamoto,^{1*} Daisuke Tamura,² Gen Nishimura,³ Keiko Shimojima,⁴ and Toshiyuki Yamamoto⁴

¹Department of Medical Genetics, Osaka Medical Center and Research Institute for Maternal and Child Health, Osaka, Japan

²Department of Orthopedics, Osaka Medical Center and Research Institute for Maternal and Child Health, Osaka, Japan

³Department of Pediatric Imaging, Tokyo Metropolitan Children's Medical Center, Tokyo, Japan

⁴Tokyo Women's Medical University Institute for Integrated Medical Sciences, Tokyo, Japan

Received 13 May 2011; Accepted 4 September 2011

We report on a patient with a submicroscopic deletion of 12q13 detected by array-CGH and confirmed by FISH. He was haploinsufficient for the *HOXC* gene cluster and some other neighboring genes. *HOX* genes have an important role in the initial formation of the body. The patient showed characteristic features including severe kyphoscoliosis, digital abnormalities, cardiac anomaly, expressive language, and global developmental delay. Radiologic features of the fingers had some similarities with those for multiple synostosis syndrome. No human genetic disorders due to *HOXC* abnormalities are yet known. We tentatively assume that his skeletal anomalies are associated with haploinsufficiency of the *HOXC* gene cluster. Further studies are necessary to determine the clinical importance of haploinsufficiency of the *HOXC* gene cluster. © 2011 Wiley Periodicals, Inc.

Key words: *HOX*; *HOXC*; array-CGH; kyphoscoliosis; multiple synostosis syndrome

INTRODUCTION

HOX genes have an important role in the initial formation of the body plan by providing positional information along the anterior–posterior body and limb axis and are associated with neural tube closure. *HOX* A, B, C, and D make a cluster on chromosomes 7, 17, 12, and 2, respectively. Each cluster consists of 9–11 genes from 13 paralogous groups. The order of the *HOX* genes along the chromosome correlates with their expression along the anterior/posterior axis of the embryo.

Some of the *HOX* genes are associated with genetic syndromes. Akarsu et al. [1996] reported that a polyalanine tract expansion in *HOXD13* causes synpolydactyly (OMIM #186000). Mortlock and Innis [1997] found a nonsense mutation in *HOXA13* among patients with hand-foot-genital syndrome (OMIM #140000). Thompson and Nguyen [2000] reported that megakaryocytic thrombocytopenia and radio-ulnar synostosis (OMIM #605432) are associated with *HOXA11* mutations. Shrimpton et al. [2004] reported a *HOXD10* mutation in a family with isolated congenital

How to Cite this Article:

Okamoto N, Tamura D, Nishimura G, Shimojima K, Yamamoto T. 2011.

Submicroscopic deletion of 12q13 including *HOXC* gene cluster with skeletal anomalies and global developmental delay.

Am J Med Genet Part A 155:2997–3001.

vertical talus and Charcot-Marie-Tooth disease (OMIM #142984). Tischfield et al. [2005] identified homozygous truncating mutations in *HOXA1* in patients with horizontal gaze abnormalities, deafness, facial weakness, hypoventilation, vascular malformations of the internal carotid arteries and cardiac outflow tract, intellectual disability, and autism spectrum disorder. Two syndromes associated with homozygous mutations of *HOXA1* are known as the Bosley-Salih-Alorainy syndrome and the Athabaskan brainstem dysgenesis syndrome (OMIM #601536) [Bosley et al., 2008]. Alasti et al. [2008] reported a mutation in *HOXA2* in autosomal-recessive microtia (OMIM #612290).

Spitz et al. [2002] reported a t(2;8)(q31;p21) balanced translocation with breakpoints near the human *HOXD* complex. The patient had mesomelic dysplasia of the upper limbs and vertebral defects. Dlugaszewska et al. [2006] reported three patients with limb abnormalities and breakpoints involving chromosome 2q31. None of the three 2q31 breakpoints, which all mapped close to the *HOXD*

Additional supporting information may be found in the online version of this article.

Grant sponsor: Ministry of Health, Labour, and Welfare in Japan.

*Correspondence to:

Dr. Nobuhiko Okamoto, Department of Medical Genetics, Osaka Medical Center and Research Institute for Maternal and Child Health, 840 Murodocho, Izumi, Osaka 594-1101, Japan. E-mail: okamoto@osaka.email.ne.jp

Published online 8 November 2011 in Wiley Online Library

(wileyonlinelibrary.com).

DOI 10.1002/ajmg.a.34324

cluster, disrupted any known genes. They suggested that the three rearrangements disturb normal *HOXD* gene regulation by position effects. Yue et al. [2007] reported a boy with severe intellectual disability, funnel chest, bell-shaped thorax, and hexadactyly of both feet. The patient had a balanced de novo t(12;17)(p13.3;q21.3) translocation. The breakpoint was near the *HOXB* cluster. They proposed that misregulation of a *HOXB* gene(s) by position effect is responsible for the patient's phenotype. Jun et al. [2011] reported a patient with the *HOXA* cluster deletion with manifestations similar to those observed in hand-foot-genital syndrome, which is caused by a haploinsufficiency of *HOXA13*.

We report on a patient with distinctive skeletal anomalies with a submicroscopic deletion of 12q13. He was haploinsufficient for the *HOXC* gene cluster. So far, no human genetic disorders due to *HOXC* abnormalities are reported. We discuss the clinical features in the patient and the haploinsufficiency of the *HOXC* genes.

CLINICAL REPORT

The 14-year-old male proband was the first-born child of a 26-year-old mother and a 30-year-old father, both healthy and non-consanguineous. After an uncomplicated pregnancy, he was born at 39 weeks of gestation by induced delivery. His length was 53 cm (90th centile). His birth weight was 3,010 g, within normal limits (25th centile). After birth, cardiac murmur was noticed. Echocardiography revealed tetralogy of Fallot. Cardiac surgery was carried out successfully at 2 years of age. Surgery for bilateral inguinal hernia and strabismus was done at 3 years of age. His dentition was abnormal. Persistent teeth erupted before the loss of primary teeth. He showed hypodontia.

His development was delayed since early infancy. From the age of 6 months, he received physical training for delayed motor development. He was able to roll over at 10 months of age, and to sit alone at 3 years of age. He started to walk independently at 5 years of age and the spine deformity appeared. His global development quotient was 20 at 3 years of age. He attended special education in school. Gradually, he could understand simple words. His intellectual quotient remained around 30 and verbal production was almost absent. However, recently he could express simple sentences using key boards.

Physical examination identified dysmorphic features, including a long face, a broad nose, prominent ears, bilateral low-set ears, downslanting palpebral fissures and a high palate. Severe kyphosis and mild scoliosis were remarkable features. The radial heads were dislocated bilaterally. Camptodactyly of middle and ring fingers, inflexible distal interphalangeal joints of index fingers and adducted thumbs of both hands were noted (Fig. 1A). Hearing and visual acuity were normal. His weight was 29 kg (<3rd centile), and his length was 160 cm (<3rd centile). His head circumference was average for his age, 14 years.

Radiographic analysis revealed severe kyphosis and mild scoliosis in the thoracic spine (Fig. 2A,B). The upper thorax was mildly narrowed. The proximal interphalangeal joints of both the middle and ring fingers showed flexion contracture with para-articular swelling (Fig. 1B). The proximal interphalangeal joints of both index fingers were swollen as well. The metacarpophalangeal joint of the right index finger and proximal interphalangeal joint of the

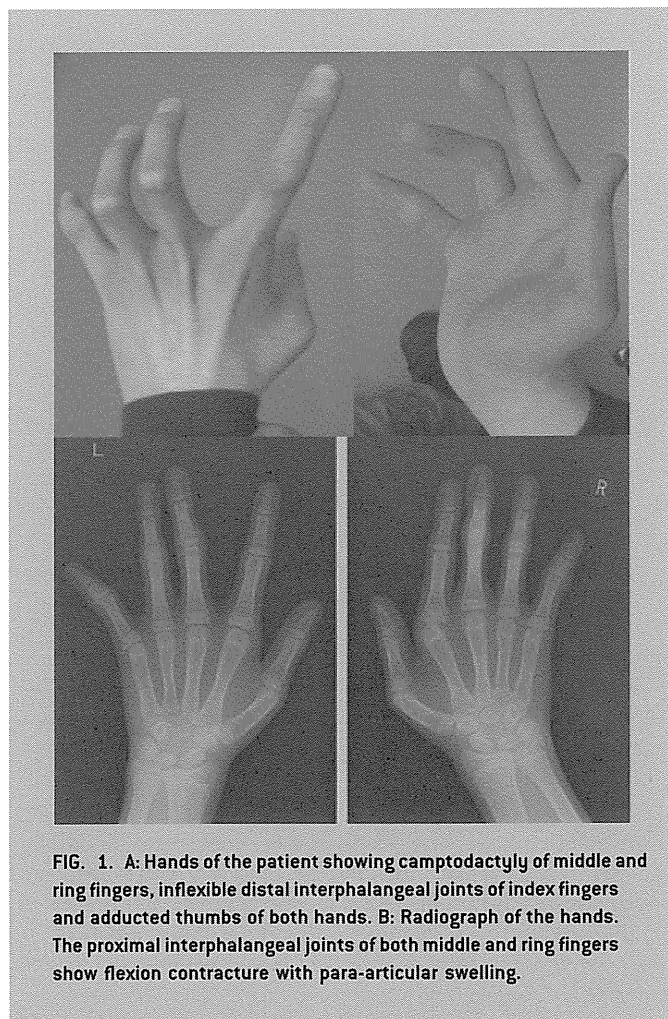


FIG. 1. A: Hands of the patient showing camptodactyly of middle and ring fingers, inflexible distal interphalangeal joints of index fingers and adducted thumbs of both hands. B: Radiograph of the hands. The proximal interphalangeal joints of both middle and ring fingers show flexion contracture with para-articular swelling.

left little finger showed ulnar deviation. The metacarpals were mildly undertubulated. Radiologic features of the fingers were like those seen in multiple synostosis syndrome. However, no carpal or tarsal coalition was found.

Results of neuroradiological examinations including brain CT and MRI were normal. Routine laboratory tests were normal. His karyotype by G-banded analysis was 46,XY. Array-CGH analyses were performed to look for submicroscopic chromosomal aberrations.

MATERIALS AND METHODS

After obtaining informed consent and the permission of the institution's ethics committee, peripheral blood samples were drawn from the patient and his parents. Genomic DNA was extracted using the QIAquick DNA extraction kit (Qiagen, Valencia, CA).

Based on the hypothesis that the patient might have submicroscopic chromosomal aberrations, array-CGH analysis was performed using the Human Genome CGH Microarray 60K (Agilent Technologies, Santa Clara, CA) as described previously [Shimojima et al., 2009].

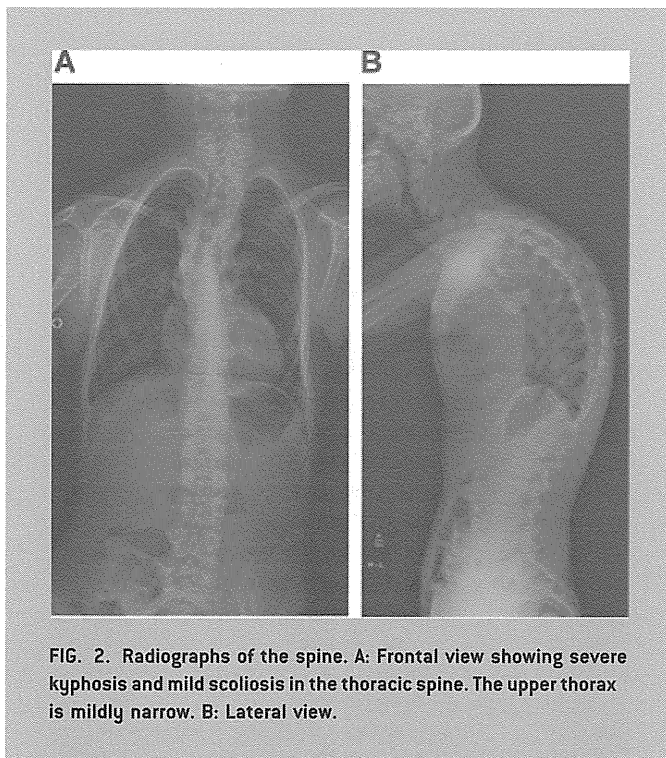


FIG. 2. Radiographs of the spine. A: Frontal view showing severe kyphosis and mild scoliosis in the thoracic spine. The upper thorax is mildly narrow. B: Lateral view.

Metaphase nuclei were prepared from peripheral blood lymphocytes by standard methods and used for FISH with human BAC clones selected from the UCSC genome browser (<http://www.genome.ucsc.edu>) as described elsewhere [Shimojima et al., 2009]. Physical positions refer to the March 2006 human reference sequence (NCBI Build 36.1).

RESULTS

By array-CGH analysis, loss of genomic copy numbers was identified in the region 12q13, which included the *HOXC* cluster (Fig. 3). The size of the deletion was 1.7 Mb. FISH analyses confirmed the deletion (see Supplementary Fig. A). FISH analyses of the parents found the deletion was de novo (data not shown). The karyotype of the patient was arr 12q13.1 (51,965,307-53,642,659)×1 dn.

DISCUSSION

A patient with distinctive skeletal anomalies had a submicroscopic deletion of 12q13 including *HOXC* gene cluster. His features included tetralogy of Fallot, abnormal dentition, and global developmental delay. This is the first report of *HOXC* gene cluster deletion. Human genetic disorders due to *HOXC* abnormalities are not known.

There have been multiple knock out studies on *Hoxc* genes. *Hoxc-4* is expressed in the most anterior regions of the CNS and prevertebral column. *Hoxc-4* mutant ($-/-$) mice showed a partial posterior homeotic transformation of the 7th cervical vertebra [Saegusa et al., 1996]. In addition, anterior transformations of

the 3rd and 8th thoracic vertebrae, and an aperture or a fissure in the xiphoid process of the sternum were observed. No obvious defects were observed in the CNS. *Hoxc-4* ($-/-$) mice manifested vertebral defects that extended from the 2nd to 11th thoracic vertebra and died because of esophageal stenosis [Boulet and Capecchi, 1996].

Hoxc-8 is expressed in the limbs, backbone rudiments, and neural tube of mouse midgestation embryos, and in the cartilage and skeleton of newborns. Le Mouellic et al. [1992] generated *Hoxc-8* ($-/-$) mice. The mice were born alive, but most of them died within a few days. Anterior transformation in the several skeletal segments was characteristic. The 8th pair of ribs attached to the sternum and the 14th pair of ribs appeared on the 1st lumbar vertebra. During embryogenesis, *Hoxc-8* is highly expressed in motoneurons within spinal cord segments C7 to T1. These motoneurons innervate forelimb distal muscles that move the forepaw. *Hoxc-8*-deficient mice showed a congenital prehension deficiency of the forepaw due to abnormal innervation [Tiret et al., 1998].

Suemori et al. [1995] generated *Hoxc-9* mutant mice. Homozygous mice showed an anterior homeotic transformation from the 10th thoracic vertebra to the first lumbar vertebra. Bending and fusion of the ribs were observed. Eight or nine pairs of ribs were attached to the sternum. The sternum showed an abnormal pattern of ossification. Phenotypes of the mutant mice resembled those of the *Hoxc-8* mutant mice. Functional interaction between *Hoxc-8* and *Hoxc-9* during segmental determination was suspected.

Godwin and Capecchi [1998] reported *Hoxc-13* expression in the nails, tail, vibrissae, and filiform papillae of the tongue, and in hair follicles throughout the body. Mice homozygous for mutant alleles of *Hoxc-13* show brittle hair resulting in alopecia.

Suemori and Noguchi [2000] produced *HoxC* cluster null ($-/-$) mice. These mice die soon after birth with minor transformations. Perinatal death of the *HoxC* cluster ($-/-$) mutant mice is thought to be attributable to a neuromuscular defect in respiratory organs. Gross appearance of the skeleton and internal organs was almost normal. The mutant mouse showed subtle vertebral and rib anomalies. Malformations in the skeleton were even milder than those observed in some single gene mutant mice of *HoxC* genes. This means that at least some genes within a cluster interact with each other. The phenotype of *HoxC* cluster ($+/-$) mice, which have a similar genetic condition to our patient, was normal.

The phenotype of knockout mice does not always correspond to human disorders. Skeletal manifestations in our patient were not evident in his early childhood. Skeletal changes may progress during growth. Interestingly, translocation breakpoint near *HOXB* and *HOXD* with positional effect caused thoracic deformities and digital abnormalities [Spitz et al., 2002; Dlugaszewska et al., 2006; Yue et al., 2007]. We tentatively assume that skeletal anomalies in our patient are associated with haploinsufficiency of the *HOXC* gene cluster.

Radiologic features of the fingers had some similarities with those for multiple synostosis syndrome (OMIM #186500). Shi et al. [1999] found that Smad1 dislodges Hoxc-8 from its DNA-binding element and result in the induction of gene expression. Bone morphogenetic proteins (BMPs) induce osteoblast differentiation and bone formation. Smad1 mediates signaling initiated by BMPs and activates osteopontin and osteoprotegerin gene expression by dislodging Hoxc-8 from its DNA-binding sites [Liu et al., 2004].

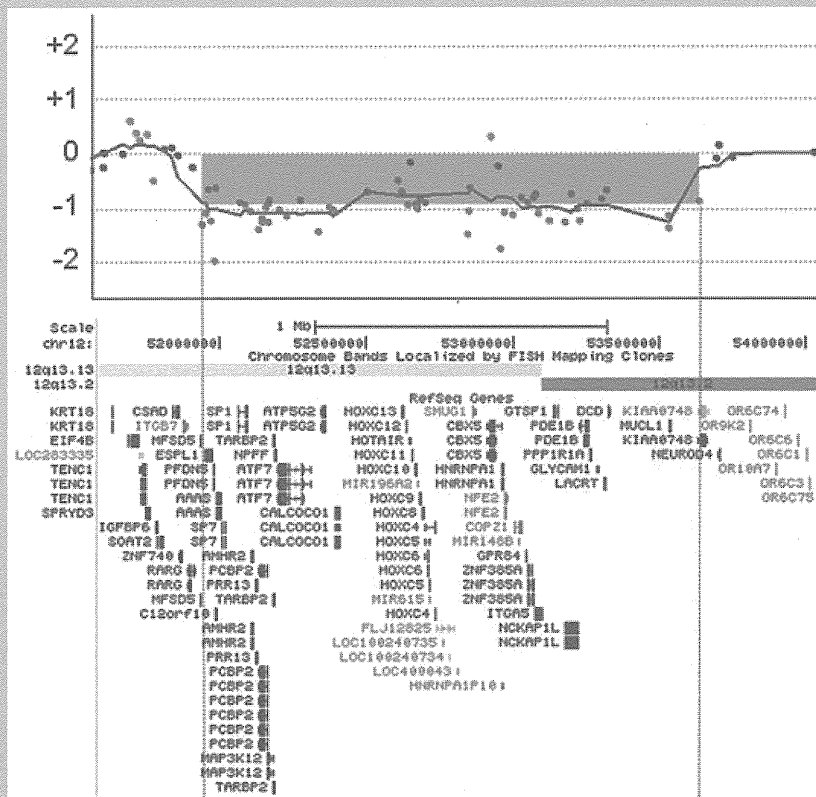


FIG. 3. Array-CGH revealed a loss of genomic copy numbers in the region 12q13, which included the *HOXC* cluster.

These findings indicate that *HOXC8* deficiency may induce osteogenesis by activating osteopontin and osteoprotegerin. The manifestations similar to the multiple synostosis syndrome, the flexion contracture and other digital abnormalities in our patient, may have some association with the *HOXC8* haploinsufficiency.

The multiple genes involved in the deletion may contribute to the manifestations. Our patient was haploinsufficient for *SP7/OSX*, *AAAS*, and *AMHR2*. Lapunzina et al. [2010] reported a homozygous single base pair deletion (c.1052delA) in *SP7/OSX* in an Egyptian child with recessive osteogenesis imperfecta (OMIM #613849). *SP7/OSX* plays a key role in human bone development. The triple-A syndrome (OMIM #231550) is caused by mutation in the gene-encoding aladin (*AAAS*; OMIM 605378). The anti-Müllerian hormone type II (*AMHR2*) receptor is the primary receptor for anti-Müllerian hormone (AMH), a protein responsible for the regression of the Müllerian duct in males. Mutations in the *AMHR2* gene lead to persistent Müllerian duct syndrome (OMIM #261550) in human males [Belville et al., 2009]. These syndromes are transmitted in autosomal recessive fashion and are not responsible for the manifestations in our patient. A haploinsufficiency of other genes may contribute to cardiac anomalies, dental anomalies, and intellectual disability with severe expressive language delay. Some of the deleted genes including *GPR84*, *PDE1B*, and *NFF* are

expressed in the nervous system. However, contribution of these genes to language development is unclear.

In conclusion, we report on a patient with distinctive skeletal anomalies and intellectual disability with a submicroscopic deletion of 12q13 including *HOXC* gene cluster. No human genetic disorders due to *HOXC* abnormalities are yet known. We posit that his kyphoscoliosis and digital abnormalities may be associated with haploinsufficiency of the *HOXC* gene cluster. Further studies of patients with similar conditions are necessary to determine the clinical significance of haploinsufficiency of the *HOXC* gene cluster.

ACKNOWLEDGMENTS

We thank for the family for their cooperation. This study was supported by the Health and Labour Research Grants in 2010 by Ministry of Health, Labour and Welfare in Japan.

REFERENCES

- Akarsu AN, Stoilov I, Yilmaz E, Sayli BS, Sarfarazi M. 1996. Genomic structure of *HOXD13* gene: A nine polyalanine duplication causes synpolydactyly in two unrelated families. *Hum Mol Genet* 5:945–952.

- Alasti F, Sadeghi A, Sanati MH, Farhadi M, Stollar E, Somers T, Van Camp G. 2008. A mutation in HOXA2 is responsible for autosomal-recessive microtia in an Iranian family. *Am J Hum Genet* 82:982–991.
- Belville C, Maréchal JD, Pennetier S, Carmillo P, Masgrau L, Messika-Zeitoun L, Galey J, Machado G, Treton D, Gonzalès J, Picard JY, Josso N, Cate RL, di Clemente N. 2009. Natural mutations of the anti-Mullerian hormone type II receptor found in persistent Mullerian duct syndrome affect ligand binding, signal transduction and cellular transport. *Hum Mol Genet* 18:3002–3013.
- Bosley TM, Alorainy IA, Salih MA, Aldhalaan HM, Abu-Amero KK, Oystreck DT, Tischfield MA, Engle EC, Erickson RP. 2008. The clinical spectrum of homozygous HOXA1 mutations. *Am J Med Genet A* 146A:1235–1240.
- Boulet AM, Capecchi MR. 1996. Targeted disruption of *hoxc-4* causes esophageal defects and vertebral transformations. *Dev Biol* 177:232–249.
- Długaszevska B, Silaharoglu A, Menzel C, Kübart S, Cohen M, Mundlos S, Tümer Z, Kjaer K, Friedrich U, Ropers HH, Tommerup N, Neitzel H, Kalscheuer VM. 2006. Breakpoints around the HOXD cluster result in various limb malformations. *J Med Genet* 43:111–118.
- Godwin AR, Capecchi MR. 1998. *Hoxc13* mutant mice lack external hair. *Genes and Dev* 12:11–20.
- Jun KR, Seo EJ, Lee JO, Yoo HW, Park IS, Yoon HK. 2011. Molecular cytogenetic and clinical characterization of a patient with a 5.6-Mb deletion in 7p15 including HOXA cluster. *Am J Med Genet Part A* 155A:642–647.
- Lapunzina P, Aglan M, Temtamy S, Caparrós-Martín JA, Valencia M, Letón R, Martínez-Glez V, Elhossini R, Amr K, Vilaboa N, Ruiz-Perez VL. 2010. Identification of a frameshift mutation in *Osterix* in a patient with recessive osteogenesis imperfecta. *Am J Hum Genet* 87:110–114.
- Le Mouellic H, Lallemand Y, Brûlet P. 1992. Homeosis in the mouse induced by a null mutation in the *Hox-3.1* gene. *Cell* 69:251–264.
- Liu Z, Shi W, Ji X, Sun C, Jee WS, Wu Y, Mao Z, Nagy TR, Li Q, Cao X. 2004. Molecules mimicking Smad1 interacting with Hox stimulate bone formation. *J Biol Chem* 279:11313–11319.
- Mortlock DP, Innis JW. 1997. Mutation of HOXA13 in hand-foot-genital syndrome. *Nat Genet* 15:179–180.
- Saegusa H, Takahashi N, Noguchi S, Suemori H. 1996. Targeted disruption in the mouse *Hoxc-4* locus results in axial skeleton homeosis and malformation of the xiphoid process. *Dev Biol* 174:55–64.
- Shi X, Yang X, Chen D, Chang Z, Cao X. 1999. Smad1 interacts with homeobox DNA-binding proteins in bone morphogenetic protein signaling. *J Biol Chem* 274:13711–13717.
- Shimajima K, Páez MT, Kurosawa K, Yamamoto T. 2009. Proximal interstitial 1p36 deletion syndrome: The most proximal 3.5-Mb microdeletion identified on a dysmorphic and mentally retarded patient with *inv(3)(p14.1q26.2)*. *Brain and Development* 31:629–633.
- Shrimpton AE, Levinsohn EM, Yozawitz JM, Packard DS Jr, Cady RB, Middleton FA, Persico AM, Hootnick DR. 2004. A HOX gene mutation in a family with isolated congenital vertical talus and Charcot-Marie-Tooth disease. *Am J Hum Genet* 75:92–96.
- Spitz F, Montavon T, Monso-Hinard C, Morris M, Ventruto ML, Antonarakis S, Ventruto V, Duboule D. 2002. A t(2;8) balanced translocation with breakpoints near the human HOXD complex causes mesomelic dysplasia and vertebral defects. *Genomics* 79:493–498.
- Suemori H, Noguchi S. 2000. Hox C cluster genes are dispensable for overall body plan of mouse embryonic development. *Dev Biol* 220:333–342.
- Suemori H, Takahashi N, Noguchi S. 1995. *Hoxc-9* mutant mice show anterior transformation of the vertebrae and malformation of the sternum and ribs. *Mech Dev* 51:265–273.
- Thompson AA, Nguyen LT. 2000. Amegakaryocytic thrombocytopenia and radio-ulnar synostosis are associated with HOXA11 mutation. *Nat Genet* 26:397–398.
- Tiret L, Le Mouellic H, Maury M, Brûlet P. 1998. Increased apoptosis of motoneurons and altered somatotopic maps in the brachial spinal cord of *Hoxc-8*-deficient mice. *Development* 125:279–291.
- Tischfield MA, Bosley TM, Salih MA, Alorainy IA, Sener EC, Nester MJ, Oystreck DT, Chan WM, Andrews C, Erickson RP, Engle EC. 2005. Homozygous HOXA1 mutations disrupt human brainstem, inner ear, cardiovascular and cognitive development. *Nat Genet* 37:1035–1037.
- Yue Y, Farcas R, Thiel G, Bommer C, Grossmann B, Galetzka D, Kelbova C, Küpferling P, Daser A, Zechner U, Haaf T. 2007. De novo t(12;17)(p13.3;q21.3) translocation with a breakpoint near the 5' end of the HOXB gene cluster in a patient with developmental delay and skeletal malformations. *Eur J Hum Genet* 15:570–577.

MBTPS2 Mutation Causes BRESEK/BRESHECK Syndrome

Misako Naiki,^{1,2} Seiji Mizuno,³ Kenichiro Yamada,¹ Yasukazu Yamada,¹ Reiko Kimura,¹ Makoto Oshiro,⁴ Nobuhiko Okamoto,⁵ Yoshio Makita,⁶ Mariko Seishima,⁷ and Nobuaki Wakamatsu^{1*}

¹Department of Genetics, Institute for Developmental Research, Aichi Human Service Center, Kasugai, Aichi, Japan

²Department of Pediatrics, Nagoya University Graduate School of Medicine, Nagoya, Aichi, Japan

³Department of Pediatrics, Central Hospital, Aichi Human Service Center, Kasugai, Aichi, Japan

⁴Department of Pediatrics, Japanese Red Cross Nagoya Daiichi Hospital, Nagoya, Aichi, Japan

⁵Department of Medical Genetics, Osaka Medical Center and Research Institute for Maternal and Child Health, Izumi, Osaka, Japan

⁶Education Center, Asahikawa Medical University, Asahikawa, Hokkaido, Japan

⁷Department of Dermatology, Gifu University Graduate School of Medicine, Gifu, Gifu, Japan

Received 25 July 2011; Accepted 17 October 2011

BRESEK/BRESHECK syndrome is a multiple congenital malformation characterized by brain anomalies, intellectual disability, ectodermal dysplasia, skeletal deformities, ear or eye anomalies, and renal anomalies or small kidneys, with or without Hirschsprung disease and cleft palate or cryptorchidism. This syndrome has only been reported in three male patients. Here, we report on the fourth male patient presenting with brain anomaly, intellectual disability, growth retardation, ectodermal dysplasia, vertebral (skeletal) anomaly, Hirschsprung disease, low-set and large ears, cryptorchidism, and small kidneys. These manifestations fulfill the clinical diagnostic criteria of BRESHECK syndrome. Since all patients with BRESEK/BRESHECK syndrome are male, and X-linked syndrome of ichthyosis follicularis with atrichia and photophobia is sometimes associated with several features of BRESEK/BRESHECK syndrome such as intellectual disability, vertebral and renal anomalies, and Hirschsprung disease, we analyzed the causal gene of ichthyosis follicularis with atrichia and photophobia syndrome, *MBTPS2*, in the present patient and identified a p.Arg429His mutation. This mutation has been reported to cause the most severe type of ichthyosis follicularis with atrichia and photophobia syndrome, including neonatal and infantile death. These results demonstrate that the p.Arg429His mutation in *MBTPS2* causes BRESEK/BRESHECK syndrome. © 2011 Wiley Periodicals, Inc.

Key words: BRESEK/BRESHECK syndrome; IFAP syndrome; *MBTPS2*; mutation; S2P

INTRODUCTION

BRESEK/BRESHECK syndrome (OMIM# 300404), a multiple congenital malformation disorder characterized by brain anomalies, intellectual disability, ectodermal dysplasia, skeletal deformities, Hirschsprung disease, ear or eye anomalies, cleft palate or

How to Cite this Article:

Naiki M, Mizuno S, Yamada K, Yamada Y, Kimura R, Oshiro M, Okamoto N, Makita Y, Seishima M, Wakamatsu N. 2011. *MBTPS2* mutation causes BRESEK/BRESHECK syndrome.

Am J Med Genet Part A .

cryptorchidism, and kidney dysplasia/hypoplasia [Reish et al., 1997]. The acronym BRESEK refers to the common findings, whereas BRESHECK refers to all manifestations. Because the first two patients were maternally related half brothers, an X-linked disorder was proposed. Although each symptom of these patients is often observed in other congenital diseases, the combination of all symptoms is rare, and only one additional patient with BRESEK has been reported to date [Tumialán and Mapstone, 2006]. Here, we present the fourth male patient with multiple anomalies. The patient presented with a variety of clinical features that were consistent with those of the previously reported BRESHECK syndrome.

The syndrome of ichthyosis follicularis with atrichia and photophobia (IFAP, OMIM# 308205), an X-linked recessive oculocutaneous disorder, is characterized by a peculiar triad of ichthyosis follicularis, total or subtotal atrichia, and varying degrees

Grant sponsor: Takeda Science Foundation; Grant sponsor: Health Labour Sciences Research Grant.

*Correspondence to:

Nobuaki Wakamatsu, Department of Genetics, Institute for Developmental Research, Aichi Human Service Center, 713-8 Kamiya-cho, Kasugai, Aichi 480-0392, Japan. E-mail: nwaka@inst-hsc.jp

Published online 00 Month 2011 in Wiley Online Library (wileyonlinelibrary.com).

DOI 10.1002/ajmg.a.34373

of photophobia [MacLeod, 1909]. Martino et al. [1992] reported a male patient with IFAP syndrome presented with short stature, intellectual disability, seizures, hypohidrosis, enamel dysplasia, congenital aganglionic megacolon, inguinal hernia, vertebral and renal anomalies, and the classic symptom triad of IFAP syndrome. This report broadened the clinical features of IFAP syndrome. It should be noted that the clinical symptoms of this patient are quite similar to those of BRESHECK syndrome, with the exception of cleft palate, cryptorchidism, and photophobia (Patient 5; Table I). The gene mutated in patients with IFAP syndrome, *MBTPS2* (GenBank reference sequence NM_015884), was identified from a variety of clinical features of IFAP syndrome, including the triad and neonatal death [Oeffner et al., 2009]. Thus, the mode of inheritance and several clinical features are common to both BRESEK/BRESHECK and IFAP syndromes. These findings prompted us to perform mutation analysis of *MBTPS2* in the present patient, resulting in the identification of a missense mutation.

MATERIALS AND METHODS

Patients

Written informed consent was obtained from the parents of the patient. Experiments were conducted after approval of the institutional review board of the Institute for Developmental Research, Aichi Human Service Center. The patient (II-1; Fig. 3) was born to a 31-year-old mother (I-2) and a 31-year-old father (I-1), both healthy Japanese individuals without consanguinity. His mother miscarried her first child at 5 weeks. The pregnancy of the patient reported here was complicated with mild oligohydramnios, and he was delivered by caesarean because of a breech position at 38 weeks of gestation. His birth weight was 1,996 g (−2.6 SD), and he measured 44 cm (−2.6 SD) in length with an occipitofrontal circumference of 32.5 cm (−0.5 SD). Apgar scores at 1 and 5 min were four and eight, respectively. The patient exhibited generalized alopecia and lacked eyelashes, scalp hair, and eyebrows (Fig. 1A). The skin on the entire body was erythematous with

TABLE I. Clinical Features of BRESEK/BRESHECK and IFAP Syndromes and *MBTPS2* Mutation

Patient	BRESEK/BRESHECK syndrome				IFAP syndrome		
	1	2	3	4	5	6	7
Clinical features							
Gender	M	M	M	M	M	M	M
Gestational age (weeks)	32	40	ND	38	30	ND	ND
Birth weight (g)	990	2,230	ND	1,996	2,040	ND	ND
Intrauterine growth retardation	+	+	ND	+	−	ND	ND
Major features							
Follicular ichthyosis	−	−	ND	−	+	+	+
Atrichia	+	+	+	+	+	+	+
Photophobia	−	−	−	+	+	+	+
Brain malformation	+	+	+	+	+	−	+
Mental and growth retardation	+	+	+	+	+	+	+
Skeletal (Vertebrate) anomalies	+	+	+	+	+	+	+
Hirschsprung disease	−	+	+	+	+	+	+
Eye malformation or	+	+	+	−	+	−	−
Large ears	+	+	+	+	+	−	−
Cleft lip/palate or	−	+	−	−	−	+	−
Cryptorchidism	+	+	−	+	−	−	−
Kidney malformation	+	+	−	+	+	+	+
Other features							
Microcephaly	+	+	+	+	+	−	+
Seizures	−	+	+	+	+	−	+
Deafness	−	+	−	+	−	−	−
Hand anomalies	+	+	+	−	+	+	+
Cardiac anomalies	−	−	+	−	−	−	+
Inguinal hernia	−	−	−	−	+	+	+
Trachea anomalies	−	−	−	+	−	−	−
Regression	−	−	−	+	−	−	−
Age	6 h d	7 y	1.5 y	8 y	3 y	9 m d	14 m d
<i>MBTPS2</i> mutation	NP	NP	NP	R429H	NP	R429H	R429H

+, present; −, not present; M, male; ND, not described; NP, not performed; h, hour; d, day; m, month; y, year; R429H, Arg429His; BRESEK/BRESHECK syndrome, (Patients 1-4); IFAP syndrome, (Patients 5-7); Patients: 1, Reish et al. [1997] patient 1; 2, Reish et al. [1997] patient 2; 3, Tumialán and Mapstone [2006]; 4, present case; 5, Martino et al. [1992]; 6, Oeffner et al. [2009] 3-III:3; 7, Oeffner et al. [2009] 3-III:4.

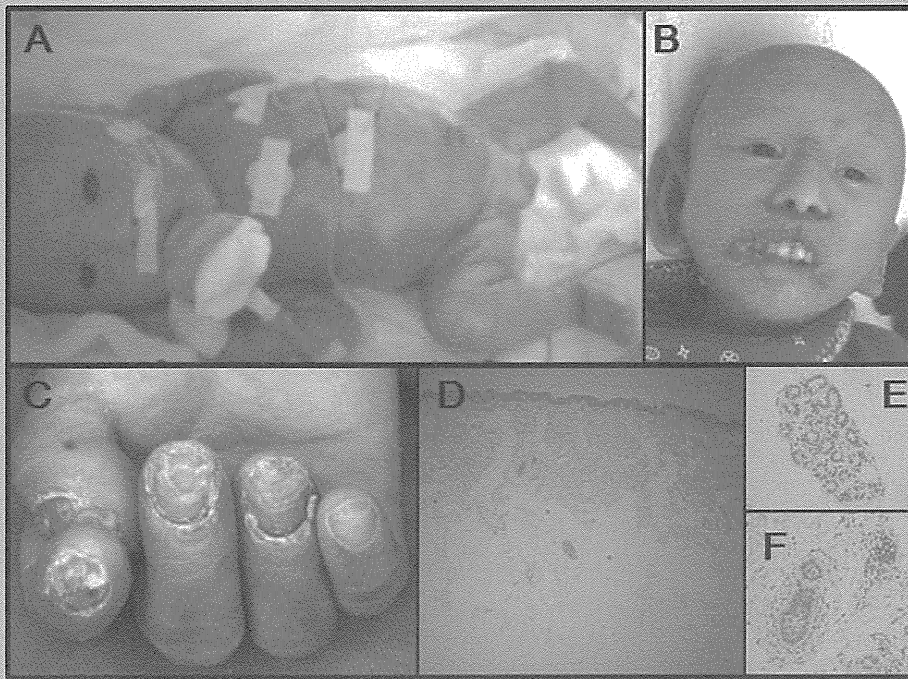


FIG. 1. Clinical appearance and dermatological findings of the patient. **A:** Lateral view of the patient at birth. Note the generalized alopecia with an absence of scalp hair, eyebrows, and eyelashes. The skin was dry and scaly, and an itchy erythema was observed over the entire body. **B:** Frontal view of the patient at 4 years of age. Note the characteristic facial appearance with long, malformed ears, a relatively high nasal bridge, and a wide nasal base. **C:** The patient had normal-sized but deformed and thickened nails. **D–F:** Histologic examination of the abdominal skin at the age of 15 months showed a reduced number of hair follicles (**D**), normal eccrine glands (**E**), and hypoplastic hair follicles (**F**).

continuous desquamation (Fig. 1A). He had malformed large ears, an inferiorly curved penis, and a bifid scrotum. The testicles were not palpable. He experienced persistent constipation, and total colonic Hirschsprung disease was confirmed through barium enema (Fig. 2E) and rectal biopsy at 2 months. A bone survey performed using three-dimensional (3D) computed tomography (CT) showed abnormal imbalanced hemivertebrae in the two lowest thoracic vertebral bodies (Fig. 2C). The patient's right kidney was smaller than normal. Brain magnetic resonance imaging (MRI) at 3 years of age demonstrated decreased volumes of the frontal and parietal lobes and thinning of the corpus callosum with dilatation of the ventricles (Fig. 2A,B). There were no abnormalities of the eyes or optic nerves. We concluded that the patient had BRESHECK syndrome. The patient had seizures at 5 months of age with an apneic episode and cyanosis. Electroencephalographic (EEG) analysis showed abnormal patterns of sharp waves in the posterior lobe. The seizures were almost completely controlled with phenobarbital. The patient was allergic to milk. At 7 months, tracheal endoscopy revealed subglottic tracheal stenosis and abnormal segmentation of the left lung. A chest CT performed at 3 years of age showed a congenital cystic adenomatoid malformation (CCAM) in the right upper lobe (Fig. 2D). Auditory brain stem responses showed bilateral 80 dB hearing loss at 8 months of age.

The patient exhibited delayed psychomotor development during his infancy. He could drink from a bottle at the age of 3 months and could sit up unsupported at 15 months. Abdominal skin biopsy at 15 months revealed reduced number of hair follicles (Fig. 1D). The eccrine glands were normal (Fig. 1E), and most of his hair follicles appeared to be hypoplastic (Fig. 1F). These findings were similar to ichthyosiform erythroderma. Photophobia was noted when the patient left the hospital and first went outside at 18 months of age. At 2 years and 6 months of age, he had a series of epileptic episodes. He experienced a maximum of 100 seizures per day, and EEG analysis showed continual abnormal spikes in the posterior lobe. The seizures were controlled with clonazepam therapy. At 2 years and 9 months of age, he could stand with support and displayed social smiles when interacting with other people. However, the patient developed psychomotor regression at the age of 3 years. He exhibited a progressive loss of emotional response to others, developed hypotonia, and could not stand or sit alone. At 4 years of age, he became bedridden and showed almost no response to people. He had highly desquamated skin, similar to that seen in ichthyosis (Fig. 1B), and easily developed erythema on the skin of the entire body. The patient had deformed and thickened nails (Fig. 1C). He had persistent corneal erosions, but ophthalmoscopy could not be performed at the age of 4 years because of corneal opacification.

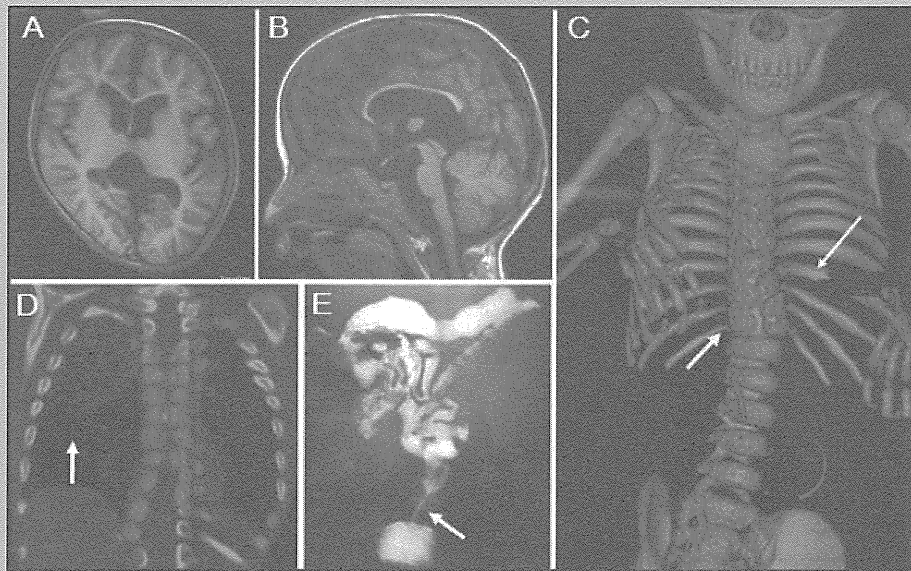


FIG. 2. CT and MRI findings of the patient. A,B: Brain MRI (T1-weighted image) at 3 years of age showed decreased volume of the cortex in the frontal and parietal lobes, the presence of a subdural cyst in the corpora quadrigemina, and dilatation of the lateral and fourth ventricle. C: A bone survey performed using 3D CT showed abnormal segmentation of the ninth rib and an imbalanced hemivertebrae in the two lowest thoracic vertebral bodies (shown with arrows). D: CT of the chest showed CCAM (Indicated by the arrow) in the right upper lobe. E: Barium enema showed a reduced caliber rectum (indicated by the arrow), suggesting that the patient had Hirschsprung disease.

Chromosomal and Molecular Genetic Studies

Genomic DNA isolated from the patient's peripheral white cells by phenol/chloroform extraction was used for *MBTPS2* mutation analysis. PCR-amplified DNA fragments were isolated using the QIAEX II Gel Extraction Kit (Qiagen, Valencia, CA) and purified using polyethylene glycol 6000 precipitation. PCR products were sequenced with the Big Dye Terminator Cycle Sequencing Kit V1.1 and analyzed with the ABI PRISM 310 Genetic Analyzer (Life Technologies, Carlsbad, CA). We also performed G-banded chromosome analysis at a resolution of 400–550 bands, genome-wide subtelomere fluorescence in situ hybridization (FISH) analysis, and array comparative genomic hybridization (array CGH) using Whole Human Genome Oligo Microarray Kits 244K (Agilent Technologies Inc., Palo Alto, CA) to identify genomic abnormalities.

RESULTS

G-banded chromosome analysis and genome-wide subtelomere FISH analyses did not show chromosomal rearrangements in the patient. Array CGH analysis did not show copy number changes in the patient's genome with the exception of known copy-number variations (CNVs). Since some patients with IFAP syndrome have been reported to present with several clinical features of BRESEK/BRESHECK syndrome, including severe intellectual disability, vertebral and renal anomalies, and Hirschsprung disease, we conducted a comprehensive sequencing analysis of all exons and intron–exon boundaries of *MBTPS2*. This analysis identified a

missense mutation (c.1286G>A, [p.Arg429His]) in exon 10, which was previously reported for IFAP syndrome (Fig. 3). The mutation was also found in one allele of the mother (I-2), indicating that the mutation was of maternal origin and that the mother was a heterozygous carrier (Fig. 3).

DISCUSSION

In this report, we describe the fourth male patient with BRESHECK syndrome in whom we identified a missense mutation (c.1286G>A, [p.Arg429His]) in *MBTPS2*, which is the causal gene for IFAP syndrome. *MBTPS2* encodes a membrane-embedded zinc metalloprotease, termed site-2 protease (S2P). S2P cleaves and activates cytosolic fragments of sterol regulatory element binding proteins (SREBP1 and SREBP2) and a family of bZIP membrane-bound transcription factors of endoplasmic reticulum (ER) stress sensors (ATF6, OASIS), after a first luminal proteolytic cut by site-1 protease (S1P) within Golgi membranes [Sakai et al., 1996; Ye et al., 2000; Kondo et al., 2005; Asada et al., 2011]. The SREBPs control the expression of many genes involved in the biosynthesis and uptake of cholesterol, whereas ATF6 and OASIS induce many genes that clean up accumulated unfolded proteins in the ER. Dysregulated SREBP activation, impaired lipid metabolism, and accumulation of unfolded proteins in the ER caused by *MBTPS2* mutations could lead to disturbed differentiation of epidermal structures, resulting in the symptom triad of IFAP syndrome [Cursiefen et al., 1999; Traboulsi et al., 2004; Elias et al., 2008]. Oeffner et al. [2009] first identified five missense mutations in *MBTPS2* in patients with IFAP

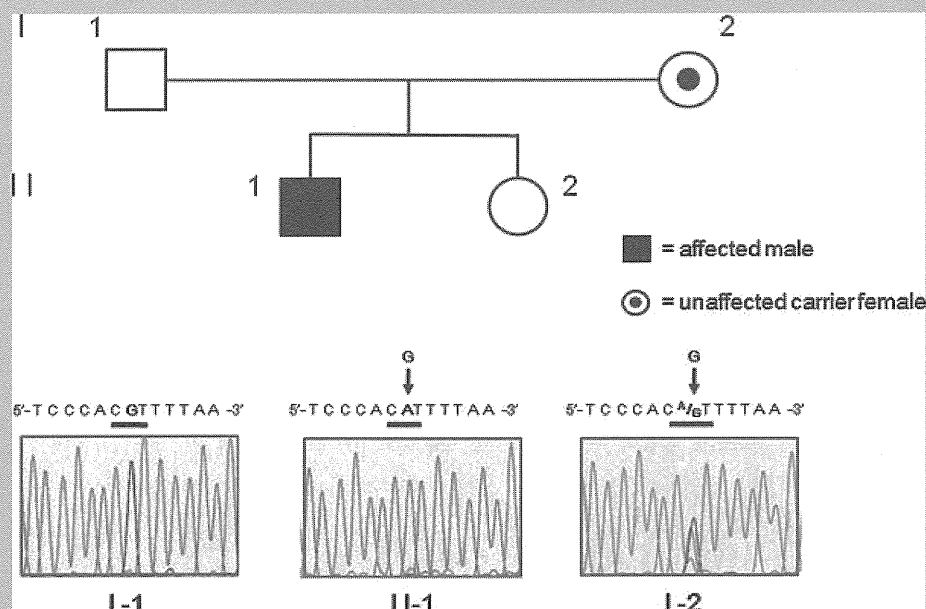


FIG. 3. Identification of a disease mutation. The sequence analyses of the patient (II-1) showed a c.1286G>A variant in exon 10 of *MBTPS2*, which predicts p.Arg429His, as indicated by the arrow (middle panel). The mother (I-2) was heterozygous for the mutation [C^A/G] (right panel).

syndrome. Transfection studies using wild type and mutant *MBTPS2* expression constructs demonstrated that the five *MBTPS2* mutations did not affect S2P protein amount and localization in the ER. However, enzyme activities, as measured by sterol responsiveness, were decreased in S2P-deficient M19 cells when the mutant *MBTPS2* was transiently expressed. Interfamilial phenotypic differences between male IFAP patients and the properties of mutants in functional assays predict a genotype–phenotype correlation, ranging from mild forms of the triad with relatively high enzyme activity (~80%) to severe manifestations of intellectual disability, various developmental defects, and early death with low enzyme activity (~15%). The identified p.Arg429His mutation in the patient reported here is one of the five missense mutations with the lowest enzyme activity. It was previously reported that all four patients harboring the p.Arg429His mutation died within 14 months of birth. The five mutations were not located in the HEIGH motif (amino acids [aa] 171–175) or in the LD₄₆₇G sequence, both of which are regions important for coordinating the zinc atom at the enzymatic active site for protease activity in the Golgi membrane [Zelenski et al., 1999]. However, among the five mutations, the p.Arg429His mutation is located closest to the intramembranous domain, and it strongly reduced the enzymatic activity and caused a severe phenotype. This finding suggests that mutations in the HEIGH motif or in the LD₄₆₇G sequence are fatal because they lead to a null function of the S2P. Although the detailed skin findings of the four patients with the p.Arg429His mutation have not been reported, it should be noted that one of the four patients (3-III:4) with the p.Arg429His mutation had brain anomaly, seizures, psychomotor retardation, vertebrae anomaly, Hirschsprung disease, absence of a kidney, atrial septum defect, and inguinal

hernia, in addition to the symptom triad of IFAP syndrome [Oeffner et al., 2009]. These symptoms overlap with the majority of symptoms observed in BRESHECK syndrome (BRESHK; six of eight symptoms observed in BRESHECK) (Table I), and the present patient has BRESHECK syndrome. Collectively, these observations suggest that the most severe form of the syndrome caused by the p.Arg429His mutation in *MBTPS2* shows features quite similar or identical to those of BRESEK/BRESHECK syndrome.

There are two major differences in the definitions of IFAP syndrome and BRESEK/BRESHECK syndrome. Ichthyosis follicularis, one of the triad symptoms of IFAP syndrome, is a clinical condition of the skin. However, several studies on IFAP syndrome have reported various skin eruptions such as psoriasis-like and ichthyosis-like eruptions [Martino et al., 1992; Sato-Matsumura et al., 2000]. In contrast, patients with BRESEK/BRESHECK syndrome showed severe lamellar desquamation with diffuse scaling [Reish et al., 1997], similar to that observed in the present patient. This could be because of the difference in features of the skin, namely, ichthyosiform erythroderma-like appearance versus ichthyosis follicularis, in patients with the most severe forms of *MBTPS2* mutation and patients with IFAP syndrome who were described earlier, respectively.

The second difference is that photophobia was not described in the reported three male patients with BRESEK/BRESHECK syndrome [Reish et al., 1997; Tumulán and Mapstone, 2006]. In the present patient, photophobia became evident after he was diagnosed with BRESHECK syndrome. Photophobia is a symptom of epithelial disturbances of the cornea, such as ulceration and vascularization, which result in corneal scarring [Traboulsi et al., 2004]. In the most severe cases of *MBTPS2* mutation, such as

patients with severe intellectual disability who are bedridden and die early, it is likely that the patients were treated in the hospital without being exposed to sunlight. Therefore, it would be difficult to observe photophobia as a main symptom in those cases. Moreover, two previously described patients with BRESEK/BRESHECK syndrome had initial maldevelopment of one eye or small optic nerves. In these patients, photophobia may not have been obvious because of malformations of the eyes and optic nerves [Reish et al., 1997]. In our study, the patient showed clinical features of BRESHECK syndrome and photophobia with *MBTPS2* mutation, indicating that the clinical features of the present patient are extremely broad compared to the features of IFAP syndrome caused by *MBTPS2* mutation that have been previously reported [MacLeod, 1909].

Recently, a missense mutation (c.1523A>G, [p.Asn508Ser]) in *MBTPS2* was identified from 26 cases of three independent families with keratosis follicularis spinulosa decalvans (KFSD; OMIM# 308800), which is characterized by the development of hyperkeratotic follicular papules on the scalp followed by progressive alopecia of the scalp, eyelashes, and eyebrows in addition to childhood photophobia and corneal dystrophy [Aten et al., 2010]. A significant association was found between KFSD and the p.Asn508Ser mutation. The specific localization of alopecia to the scalp, eyelashes, and eyebrows and the limited childhood photophobia of KFSD indicate that KFSD has a relatively mild phenotype. The authors postulate that IFAP syndrome and KFSD are within the spectrum of one genetic disorder with a partially overlapping phenotype and propose that a new name should be chosen for KFSD/IFAP syndrome with an *MBTPS2* mutation. In contrast, the BRESHECK syndrome observed in the present patient has a severe phenotype caused by the p.Arg429His mutation. The present patient and the two patients (3-III:3 and 3-III:4) with the p.Arg429His mutation displayed broader clinical features, including eight features (BRESHECK) and six features (RESHCK and BRESHK) of BRESEK/BRESHECK syndrome, respectively (patients 4, 6, and 7; Table I) [Oeffner et al., 2009]. There is a debate regarding whether the two patients harboring six features were correctly diagnosed with BRESEK/BRESHECK syndrome since the patients did not have “BRESEK” but rather a combination of six other clinical features. To better understand and clearly distinguish the clinical features of the present patient from those of the reported patients with *MBTPS2* mutations, we propose the nomenclature of “BRESHECK/IFAP syndrome” for the present patient because he has clinical features of BRESHECK syndrome. We also suggest that the BRESHECK/IFAP syndrome be used for a broader definition that would include patients harboring most features of BRESHECK syndrome, including the previously reported two patients (3-III:3 and 3-III:4) with p.Arg429His mutation in *MBTPS2* [Oeffner et al., 2009]. Data from further genetic and clinical studies on more patients are required to determine which genes or *MBTPS2* mutations are associated with BRESEK/BRESHECK or BRESHECK/IFAP syndrome, respectively.

ACKNOWLEDGMENTS

We thank the patient and his family for participating in the study. This study was supported by the Takeda Science Foundation

(to N.W.) and by the Health Labour Sciences Research Grant (to S.M. and N.W.).

REFERENCES

- Aten E, Brasz LC, Bornholdt D, Hooijkaas IB, Porteous ME, Sybert VP, Vermeer MH, Vossen RH, van der Wielen MJ, Bakker E, Breuning MH, Grzeschik KH, Oosterwijk JC, den Dunnen JT. 2010. Keratosis follicularis spinulosa decalvans is caused by mutations in *MBTPS2*. *Hum Mutat* 31:1125–1133.
- Asada R, Kanemoto S, Kondo S, Saito A, Imaizumi K. 2011. The signalling from endoplasmic reticulum-resident bZIP transcription factors involved in diverse cellular physiology. *J Biochem* 149:507–518.
- Cursiefen C, Schlötzer-Schrehardt U, Holbach LM, Pfeiffer RA, Naumann GOH. 1999. Ocular findings in ichthyosis follicularis, atrichia, and photophobia syndrome. *Arch Ophthalmol* 117:681–684.
- Elias PM, Williams ML, Holleran WM, Jiang YJ, Schmutz M. 2008. Pathogenesis of permeability barrier abnormalities in the ichthyoses: Inherited disorders of lipid metabolism. *J Lipid Res* 49:697–714.
- Kondo S, Murakami T, Tatsumi K, Ogata M, Kanemoto S, Otori K, Iseki K, Wanaka A, Imaizumi K. 2005. OASIS, a CREB/ATF-family member, modulates UPR signalling in astrocytes. *Nat Cell Biol* 7:186–194.
- MacLeod JMH. 1909. Three cases of ‘ichthyosis follicularis’ associated with baldness. *Br J Dermatol* 21:165–189.
- Martino F, D’Eufemia P, Pergola MS, Finocchiaro R, Celli M, Giampà G, Frontali M, Giardini O. 1992. Child with manifestations of dermatotrichic syndrome and ichthyosis follicularis alopecia photophobia (IFAP) syndrome. *Am J Med Genet* 44:233–236.
- Oeffner F, Fischer G, Happle R, König A, Betz RC, Bornholdt D, Neidel U, Boente Mdel C, Redler S, Romero-Gomez J, Salhi A, Vera-Casaño A, Weirich C, Grzeschik KH. 2009. IFAP syndrome is caused by deficiency in *MBTPS2*, an intramembrane zinc metalloprotease essential for cholesterol homeostasis and ER stress response. *Am J Hum Genet* 84:459–467.
- Reish O, Gorlin RJ, Hordinsky M, Rest EB, Burke B, Berry SA. 1997. Brain anomalies, retardation of mentality and growth, ectodermal dysplasia, skeletal malformations, Hirschsprung disease, ear deformity and deafness, eye hypoplasia, cleft palate, cryptorchidism, and kidney dysplasia/hypoplasia (BRESEK/BRESHECK): New X-linked syndrome? *Am J Med Genet* 68:386–390.
- Sakai J, Duncan EA, Rawson RB, Hua X, Brown MS, Goldstein JL. 1996. Sterol-regulated release of SREBP-2 from cell membranes requires two sequential cleavages, one within a transmembrane segment. *Cell* 85:1037–1046.
- Sato-Matsumura KC, Matsumura T, Kumakiri M, Hosokawa K, Nakamura H, Kobayashi H, Ohkawara A. 2000. Ichthyosis follicularis with alopecia and photophobia in a mother and daughter. *Br J Dermatol* 142:157–162.
- Traboulsi E, Waked N, Mégarbané H, Mégarbané A. 2004. Ocular findings in ichthyosis follicularis–alopecia–photophobia (IFAP) syndrome. *Ophthalmol* 25:153–156.
- Tumialán LM, Mapstone TB. 2006. A rare cause of benign ventriculomegaly with associated syringomyelia: BRESEK/BRESHECK syndrome. Case illustration. *J Neurosurg* 105:155.
- Ye J, Rawson RB, Komuro R, Chen X, Davé UP, Prywes R, Brown MS, Goldstein JL. 2000. ER stress induces cleavage of membrane-bound ATF6 by the same proteases that process SREBPs. *Mol Cell* 6:1355–1364.
- Zelenski NG, Rawson RB, Brown MS, Goldstein JL. 1999. Membrane topology of S2P, a protein required for intramembranous cleavage of sterol regulatory element-binding proteins. *J Biol Chem* 274:21973–21980.

Clinical and Genomic Characterization of Siblings With a Distal Duplication of Chromosome 9q (9q34.1-qter)

Seiji Mizuno,^{1*} Daisuke Fukushi,² Reiko Kimura,² Kenichiro Yamada,² Yasukazu Yamada,² Toshiyuki Kumagai,³ and Nobuaki Wakamatsu²

¹Department of Clinical Genetics, Central Hospital, Aichi Human Service Center, Kasugai, Japan

²Department of Genetics, Institute for Developmental Research, Aichi Human Service Center, Kasugai, Japan

³Department of Pediatric Neurology, Central Hospital, Aichi Human Service Center, Kasugai, Japan

Received 21 July 2010; Accepted 23 May 2011

We report herein on two female siblings exhibiting mild intellectual disability, hypotonia in infancy, postnatal growth retardation, characteristic appearance of the face, fingers, and toes. Their healthy mother had a translocation between 9q34.1 and the 13pter. FISH and array CGH analysis demonstrated that the two children had an additional 8.5 Mb segment of the 9q34.1-qter at 13pter. The clinical features of the present cases were similar to those of previously reported 9q34 duplication cases; however, the present cases did not exhibit other abnormal behaviors, such as autistic features or attention deficit disorders, those are reportedly associated with 9q34 duplications. A 3.0 Mb region (9q34.1-q34.3) within 9q34 duplication in our patients are overlapped with duplication region of previously reported cases and is proposed to be critical for the presentation of several phenotypes associated with 9q34 duplications. © 2011 Wiley-Liss, Inc.

Key words: 9q34 duplication; intellectual disability; array CGH; dysmorphism

INTRODUCTION

Duplications of a distal region of the long arm of chromosome 9 (9q34) are rare and few cases have been reported. The first association between 9q34 duplications and phenotypic abnormalities were demonstrated in seven cases in a large pedigree [Allderdice et al., 1983]. The patients had low birth weight, initial poor feeding and thriving, slight psychomotor retardation, characteristic appearance of the face, fingers, and toes. Hyperactive behavior, heart murmur, and ptosis and strabismus were also noted. In another case, a girl of 3 years and 2 months carried a 9q34 duplication and a deletion of 3p26-pter due to a balanced translocation in her mother [Hodou et al., 1987]. This patient presented with dolichocephaly, characteristic facial appearance, and long thin fingers and toes, all of which are phenotypes noted in previous cases of 9q34 duplication; she also exhibited features associated with 3p terminal monosomy. In addition, duplication of 9q34-qter and monosomy of a small region on 12p13.3 in a male infant was described by Spinner et al. [1993]. The same patient was followed up at 18 years of age, and the duplicated and deleted regions were determined in detail by

How to Cite this Article:

Mizuno S, Fukushi D, Kimura R, Yamada K, Yamada Y, Kumagai T, Wakamatsu N. 2011. Clinical and genomic characterization of siblings with a distal duplication of chromosome 9q (9q34.1-qter). *Am J Med Genet Part A* 9999:1–7.

array-based comparative genomic hybridization (array CGH) analysis [Youngs et al., 2010]. The patient exhibited autistic features, hyperactivity, and attention deficit disorder in addition to the features associated with 9q34 duplications reported previously. Gawlik-Kuklinska et al. [2007] reported the case of a 17-year-old girl with an interstitial 7.4 Mb duplication of 9q34.1-q34.3 determined by array CGH analysis and compared the clinical features of the patient with those of previous cases. This patient exhibited the features common to patients with 9q34 duplications and three additional phenotypes of food-seeking behavior, obesity, and secondary amenorrhea.

In this report, we present two female siblings with 9q34.1-qter duplications and compare the clinical features and 9q34 duplication region of these patients with those of two previously reported cases using array CGH analysis. We also discuss the loci potentially responsible for the several phenotypes associated with a specific segment of 9q34.

Additional supporting information may be found in the online version of this article.

Grant sponsor: Takeda Science Foundation; Grant sponsor: Health Labour Sciences Research Grant.

*Correspondence to:

Seiji Mizuno, Aichi Human Service Center, Department of Pediatrics, Central Hospital, Kasugai, Japan. E-mail: seiji_mizuno@aichi-colony.jp

Published online 8 August 2011 in Wiley Online Library (wileyonlinelibrary.com).

DOI 10.1002/ajmg.a.34160